Journal of Innovative Technology, Vol. 8, No. 2, pp. 97-118, September 2026
http://doi.org/10.29424/JIT.202609_8(2).0009

Metaheuristic-Based Harmonic Parameter Estimation in Smart Power Systems Using Salp Swarm Optimization

Khalid Mehmood Cheema [1*], Khizer Mehmood [2], Naveed Ishtiaq Chaudhary [3]

ABSTRACT

The transition of conventional power systems into modern and smart systems is being carried out to improve reliability and power quality and integrate renewable energy sources. The power quality issue has attracted significant attention because electronic devices and renewable energy sources are integrated with nonlinear loads into modern and smart power systems. The power electronic devices and nonlinear loads cause severe harmonic generation in the power system; therefore, accurate estimation and elimination are necessary for the smooth and efficient working of power systems with appropriate power quality. Consequently, this paper proposes the Salp Swarm Algorithm (SSA) for sustainable power systems harmonic estimation for boisterous and dynamic power signals. The proposed SSA is evaluated against five well-established metaheuristic optimization algorithms under multiple noise levels, population sizes, and iteration settings. The results demonstrate that SSA consistently achieves the lowest fitness values and more accurate harmonic parameter estimates, while exhibiting faster convergence and lower computational time than the benchmark algorithms. These findings confirm the suitability of SSA for robust harmonic parameter estimation in smart power systems.

Keywords: Slap Swarm Algorithm; Harmonic Estimation; Power System; Sustainable Power; Power Quality

1. INTRODUCTION

The transformation of the conventional grid system into the smart grid continues rapidly, and many countries have transformed large parts of the conventional grid into smart grids. Renewable energy source-based power generation units are crucial to the smart grid [1]. However, these distributed power generation units cause severe power reliability issues due to the power signal harmonics generated by various system components, such as rectifiers, discharge lighting, saturated electric machines, converters, and HVDC transmission equipment [2-4]. Harmonics increase the risk of problems such as corona loss, eddy-current loss, skin effect, electromagnetic interference, protection device failure, etc. Therefore, considering these problems, it is necessary to develop an accurate, robust, effective, and simple solution mechanism to assess the quality of generated power signals. Upon the completion of an accurate estimation of harmonic parameters, it is necessary to incorporate efficient filters and compensators to suppress the effects of harmonics [5, 6].

The harmonic parameter estimation problem is a dynamic, linear, nonlinear, multimodal, and complex problem [7]. Therefore, scientists and researchers have tried to solve the harmonic parameter estimation problem by developing various statistical, mathematical, and heuristic methods [8, 9]. The power system harmonics are interpreted in phase and amplitude; however, the true model of power system harmonics consists of linear and nonlinear estimation of amplitude and phase, respectively [10].

According to available literature, it is concluded that several solution techniques are available for harmonic estimation, such as mathematical solution techniques [11], artificial intelligence solution techniques [12], and statistical solution techniques [13]. Considering the mathematical solution techniques, the discrete Fourier transform, fast Fourier transform, and Fourier transform were used for power system harmonic parameter estimation [14]. However, these techniques only apply to static signals and cannot effectively control the spectral leakage, aliasing, and picket fence effect. On the other hand, artificial intelligence techniques such as fuzzy logic [15], neural networks [16], and expert systems [17] are used for harmonic estimation, but their results are only partially accurate. Consequently, statistical methods such as least mean square [18], Kalman filter recursive least square [19], and linear least square [20] can also be applied with minor modifications, and they slightly improve results compared with the above-mentioned techniques. However, these techniques require detailed information on the observation system and the components of the fundamental frequency. Moreover, in order to achieve an accurate estimation, fine-tuning is necessary. Subsequently, in [21], researchers proposed a Kalman filter based on the local ensemble method for harmonic estimation, whereas in [22], the authors proposed the Kalman filter with the least squares error.

Similarly, in [23], the authors proposed a Kalman filter with least mean square on a phase-locked loop methodology for harmonic estimation. In [24], passive congregation and particle swarm optimization are used for the harmonic estimation. Simi-

Manuscript received June 21, 2026; revised August 11, 2026; accepted August 27, 2026.

[1*] Assistant Professor (corresponding author), Department of Electronic Engineer-ing, Fatima Jinnah Women University, Rawalpindi 46000, Pakistan.
(email: khalid.mehmood@fjwu.edu.pk)

[2] Assistant Professor, Department of Electrical Engineering, International Islamic University, Islamabad, Pakistan..

[3] Associate Professor, Graduate School of Intelligent Data Science, National Yun-lin University of Science and Technology, Taiwan R.O.C.

larly, sparse Bayesian learning algorithm [25], Modified Artificial Bee Colony [26], Gravity Search Algorithm [27], Evolutionary Backtracking Search Algorithm [28], Marine Predator Algorithm [29], Fractional Order Swarm Intelligence [30], sub-synchronous oscillations parameter estimator [31], and Ant Lion Algorithm [32] are applied for the estimation of distorted signals.

Distributed generator units and modern power grids are highly complex and challenging power systems because they incorporate sensitive and nonlinear devices, subtle loads, and complex distribution and utilization structures, which severely affect accurate estimation by the above-mentioned techniques [33-36]. Therefore, research continues to develop an accurate and suitable solution for harmonic estimation possessing specific characteristics such as adaptability, efficiency, lower complexity, and high flexibility. However, using traditional computational methods, the harmonic estimation of modern power systems at varying DC levels, variable noise levels, and significantly large search dimensions is inaccurate, complex, and inflexible. Therefore, these optimization problems can be solved using new and advanced heuristic techniques. Modern bio-inspired metaheuristics have been developed and effectively applied to solve various engineering problems [37]. The Salp Swarm Algorithm (SSA) is an advanced heuristic technical tool that has the capability to solve extensive search-dimensional, complex, and nonlinear problems.

Despite recent advances in optimization-based harmonic estimation methods, several problems remain unsolved. Some of the currently available approaches require careful parameter tuning, have premature convergence, or compromise estimation accuracy when attempting nonlinear search spaces or different levels of noise [38]. Furthermore, there have been several bio-inspired optimization techniques explored for solving the problem of harmonic parameter estimation; however, little research has been done to apply the Salp Swarm Algorithm (SSA) to this problem. The main features of SSA are adaptive leader-follower search and a balance between exploration and exploitation, making it suitable for optimization in the complex environments of a power system for estimating the harmonic amplitudes and phase angles. Thus, timely and valuable evaluation of SSA in harmonic parameter estimation is of great importance for assessing its effectiveness and applicability [39].

Based on these observations, this research aims to explore the use of Salp Swarm Algorithm for estimation of the harmonic parameters in smart power systems under various operating conditions. While studies focused on the optimization of the SSA are still possible, this paper addresses another important issue: testing the capacity of the original formulation of the SSA to solve the nonlinear harmonic estimation problem and comparing its performance with some of the state-of-the-art metaheuristics [40]. To thoroughly examine the accuracy of the estimation, convergence behavior, and computational efficiency under the proposed framework, the proposed framework is tested with different Gaussian noise levels, population sizes, and iteration numbers. The results are useful for understanding the feasibility of SSA to estimate the harmonic parameters and serve as a good performance reference for future developments in optimization-based power quality evaluation [41].

Besides these, the main focus of this research is to develop and present a framework based on SSA for solving the harmonic estimation problem in an effective, accurate, least complex, and rapid manner. The suitable balance between exploitation and exploration makes it simple and convenient for SSA to solve the complex nonlinear approximation of power system harmonics. The simulation analysis and comparison with other heuristics depict that the proposed SSA's efficiency, accuracy, and convergence time are fairly better than other heuristics. Furthermore, the remaining paper is arranged as follows. The system model is presented in Section 2, whereas the proposed heuristic is explained in Section 3. The simulation results and their discussion are presented in Section 4, while Section 5 concludes this study and explains the outcomes.

2. SYSTEM MODEL

The sinusoidal signal with multiple frequency elements, such as amplitude γ , phase ε , and angular frequency f can be stated as:

$$h(t) = \gamma_1 \sin(f_1 t + \varepsilon_1) + \gamma_2 \sin(f_2 t + \varepsilon_2) + ,...., + \gamma_n \sin(f_n t + \varepsilon_n) \quad (1)$$

Incorporating the noise $\eta(t)$ in equation (1), the above equation can be written as:

$$h(t) = \sum_{k=1}^{n} \gamma_k \sin(f_k t + \varepsilon_k) + \eta(t) \quad (2)$$

The signal in equation (2) is sampled with j period $t_j = dj$ and $h(t_j) = h(j)$gives

$$h(j) = \sum_{k=1}^{n} \gamma_k \sin(f_k j + \varepsilon_k) + \eta(j) \quad (3)$$

Consequently, by applying the trigonometric function sin $(a+b)$=sin a cos$b$+cos$a$sin$b$ into equation (3), the result is as follows:

$$h(j) = \sum_{k=1}^{n} \left[\gamma_k \{ \sin(f_k j) \cos \varepsilon_k + \cos(f_k j) \sin \varepsilon_k \} \right] + \eta(j) \quad (4)$$

Now it can be assumed that

$$w_k = \gamma_k \cos \varepsilon_k \quad (5)$$

and

$$z_k = \gamma_k \sin \varepsilon_k \quad (6)$$

Placing equations (5) and (6) into equation (4), the result is as follows:

$$h(j) = \sum_{k=1}^{n} \left[w_k \sin(f_k j) + z_k \cos(f_k j) \right] + \eta(j) \quad (7)$$

Subsequently, the intermediate parameter vector is presented in (8), the information parameter vector in (9), and the model for identification is presented in (10) and (11)

$$\Phi = \left[w_1, z_z, w_2, z_2, ..., w_k, z_k \right] \quad (8)$$

$$\Psi(j) = \left[\sin(f_1 j), \cos(f_1 j), \sin(f_2 j), \cos(f_2 j), ..., \sin(f_k j), \cos(f_k j) \right] \quad (9)$$

$$\gamma_k = \sqrt{(w_k)^2 + (z_k)^2} \quad (10)$$

$$\varepsilon_k = \tan^{-1} \frac{z_k}{w_k} \quad (11)$$

The intermediate parameters are used from equations (10) and (11) to find the actual parameters, such as phase and ampli-

tude. Moreover, the criterion function is based on the difference between *h(j)* and *h'(j)* signal, and it can be expressed as:

$$\chi(j) = \text{mean}\left[h(j) - h'(j)\right]^2 = \left[h(j) - \Psi^T(j)\Phi'\right]^2 \tag{12}$$

3. OPTIMIZATION TECHNIQUE: SALP SWARM OPTIMIZATION

The Salp Swarm Algorithm (SSA) is a recently introduced bio-inspired metaheuristic with well-established benefits over its counterparts. Therefore, the research community has exploited the optimization strength of the SSA to solve different problems, such as classification, renewable energy, wind speed forecasting, fault prediction, optimal power flow, and global optimization problems. The governing relations of the SSA are:

$$U_i = \begin{pmatrix} u_1^1 & u_2^1 & \cdots & u_g^1 \\ u_1^2 & u_2^2 & \cdots & u_g^2 \\ \vdots & \vdots & \cdots & \vdots \\ u_1^k & u_2^k & \cdots & u_g^k \end{pmatrix} \tag{13}$$

$$s_k^1 = \begin{cases} r_k + v_1((pq_k - lq_k)v_2 + lq_k) & v_3 \geq 0 \\ r_k + v_1((pq_k - lq_k)v_2 + lq_k) & v_3 < 0 \end{cases} \tag{14}$$

where s_k^1 the is the position of the first salp in the kth dimension, and r_k is the food position in the kth dimension. lq_k and pq_k represent the lower bound and the upper bound of the kth dimension, respectively, and the coefficient v_1 is calculated by (15). v_2 and v_3 are random numbers between [0,1].

$$v_1 = 2e^{-\left(\frac{4l}{Q}\right)^2} \tag{15}$$

where l shows the current iteration and Q depicts the maximum iterations. Additionally, the coefficient v_1 is a significant SSA parameter because it keeps the balance between exploitation and exploration throughout the whole search process. Concerning the followers, Eq. 16 demonstrates the update of their positions:

$$s_k^m = \frac{1}{2}\xi t^2 + \delta_0 t \tag{16}$$

where $m \geq 2$, s_k^m refers to the position of the mth salp in the kth dimension; the initial speed is denoted by δ_0, time is denoted by, and $\xi = \frac{\delta_{final}}{\delta_0}$,where $\delta = \frac{x - x_0}{t}$. Moreover, in optimization scenarios, the time depicts the iterations. Therefore, the inconsistency between the iterations can be stated as equal to 1. Furthermore, suppose that δ_0=0, then the following equation can be used to solve the problem.

$$s_k^m = \frac{1}{2}\left(s_k^m + s_k^{m-1}\right) \tag{17}$$

where $m \geq 2$. If few salps goes out of the search area, equation (18) can be used to bring them back into the search area.

$$s_k^m = \begin{cases} l^k & \text{if } s_k^m \leq l^k \\ c^k & \text{if } s_k^m \geq c^k \\ s_k^m & \text{otherwise} \end{cases} \tag{18}$$

In addition to the above details, Fig. 1 depicts the main steps of the SSA algorithm in a pictorial flowchart.

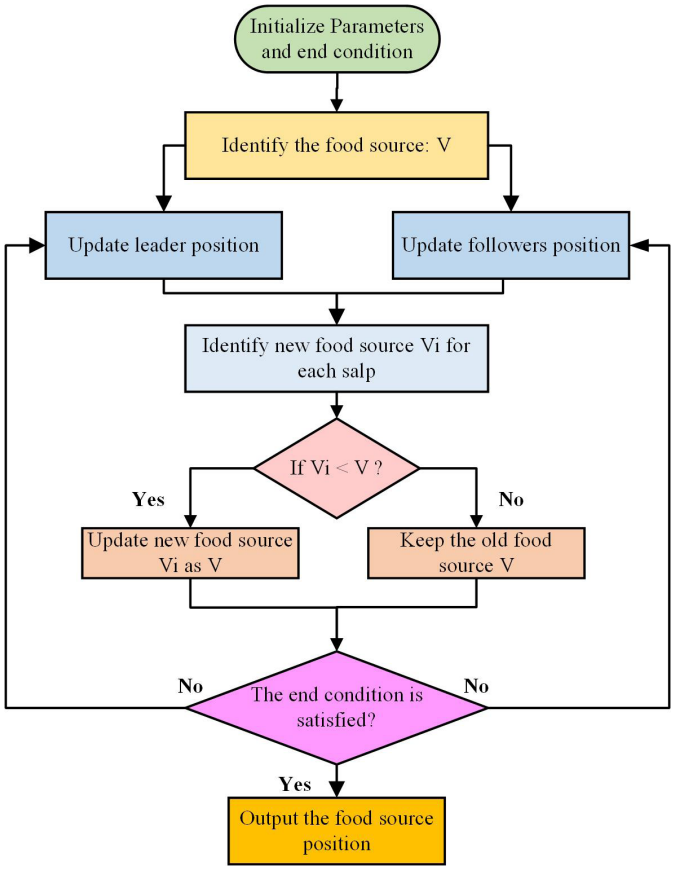
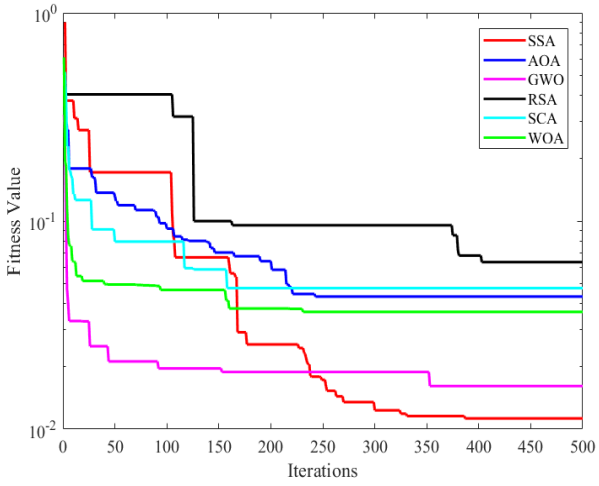


Fig. 1 Flowchart of the salp swarm algorithm

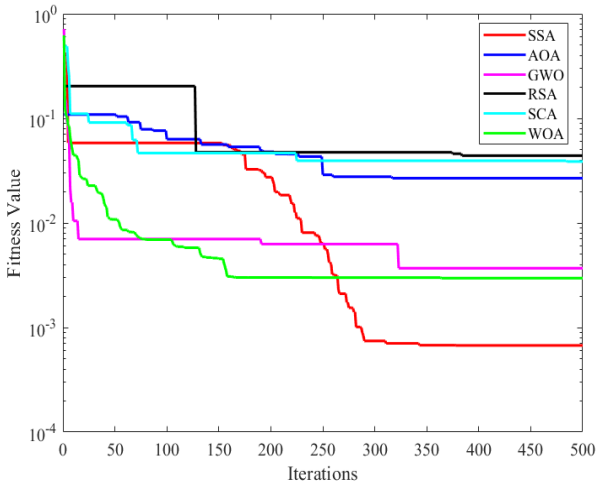
4. RESULTS AND DISCUSSION

The SSA is applied to the power system model for precise and efficient estimation of harmonics in the power signal. The simulation test is performed in MATLAB with the signal frequency set to 2kHz. Moreover, white Gaussian noise is incorporated at four levels, N_e = 20dB, 40dB, 60dB, and 80 dB, to assess the accuracy and robustness of the system model for real-time cases. Consequently, for each case, the iteration size is set to three i.e. I_t= 500, 1000, and 2000, while the population size is also set to three i.e., P_n = 30, 60, and 90 to evaluate the system behavior under various conditions. The algorithm parameters are adjusted analytically with utmost care based on the understanding and experience of optimization problems to guarantee the best performance. Therefore, the considered harmonic signal is as follows:

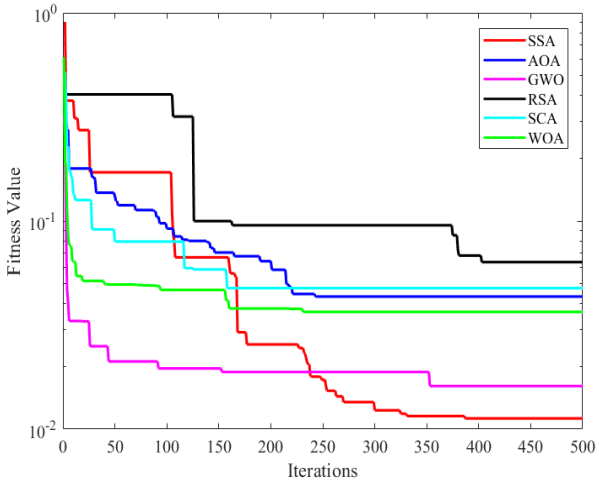
$$\begin{aligned} y(t) &= 1.5\,sin(2\times f_1\times t + 1.396) + 0.5\,sin(2\times f_3\times t + 1.047) \\ &+ 0.2\,sin(2\times f_5\times t + 0.785) + 0.15\,sin(2\times f_7\times t + 0.628) \\ &+ 0.1\,sin(2\times f_{11}\times t + 0.523) \end{aligned} \tag{19}$$



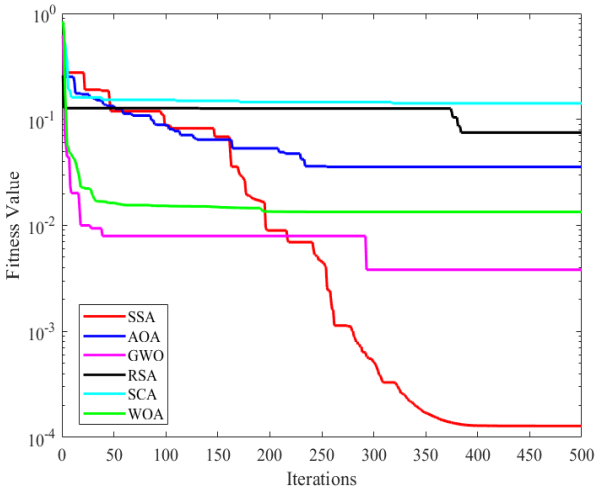
(a) N_e=20dB



(b) N_e=40dB

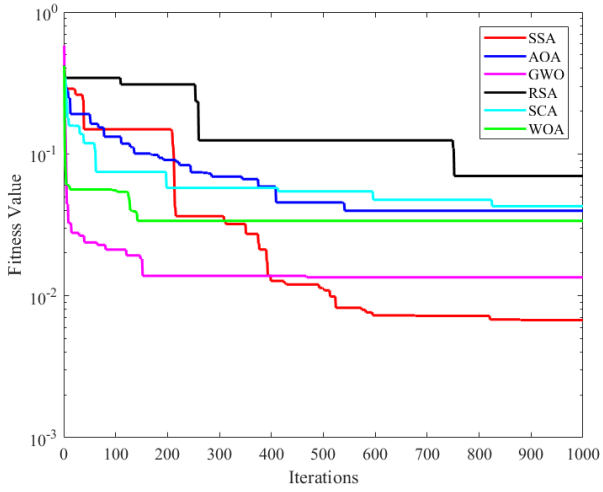


(c) N_e=60dB

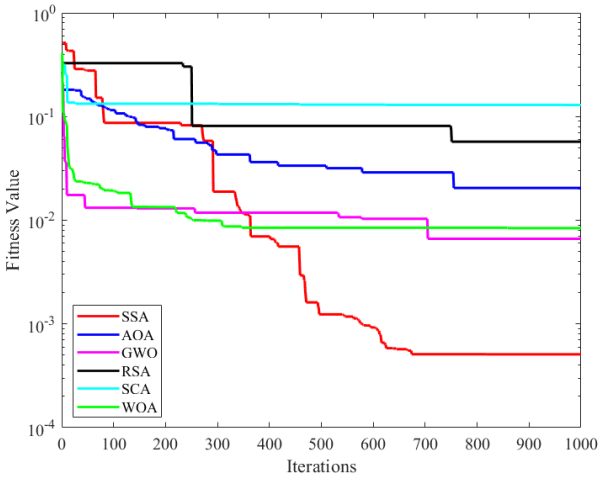


(d) N_e=80dB

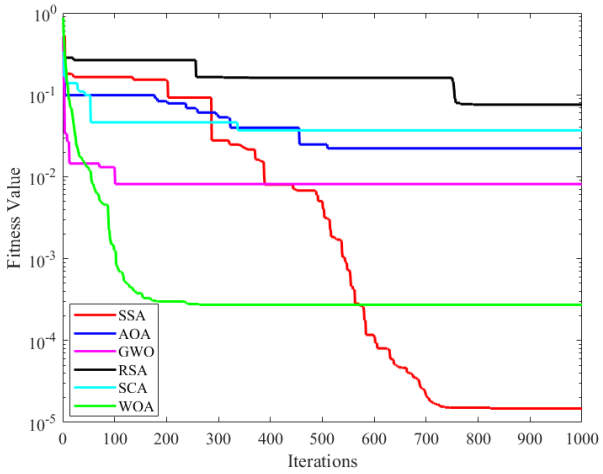
Fig. 2 Convergence plot of SSA, AOA, GWO, RSA, SCA, and WOA at P_n=90 and I_t=500



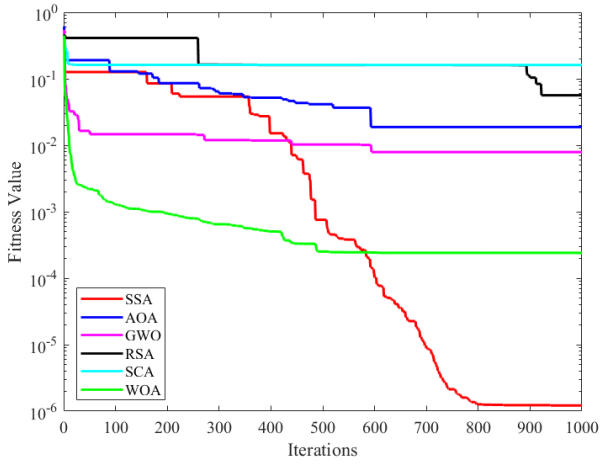
(a) N_e=20dB



(b) N_e=40dB

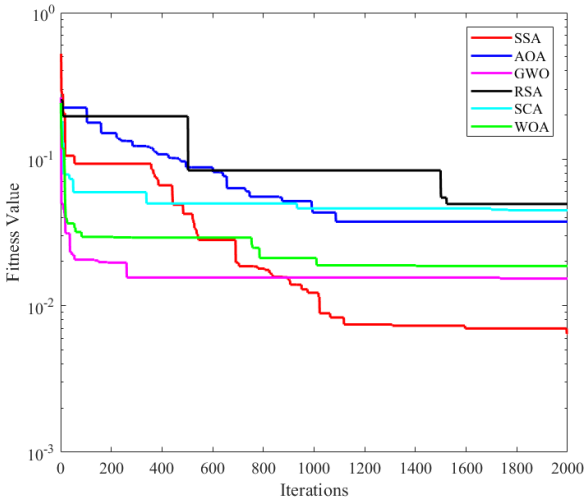


(c) N_e=60dB

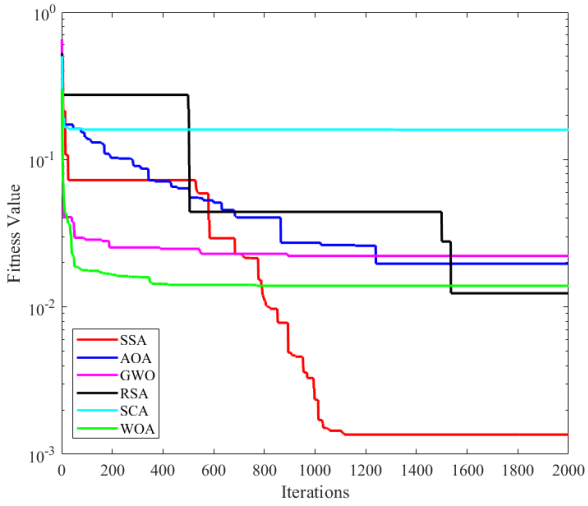


(d) N_e=80dB

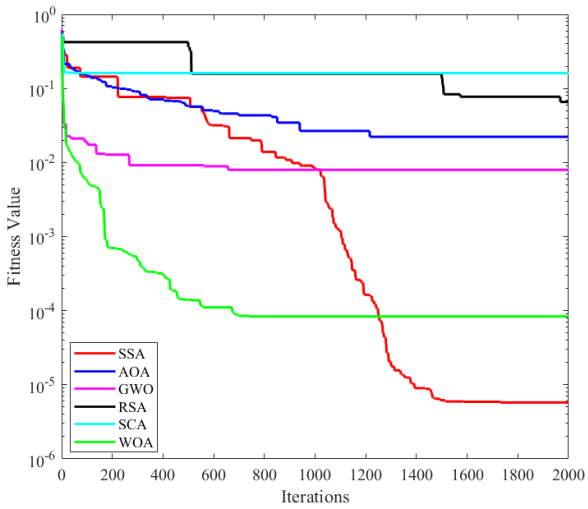
Fi. 3 Convergence plot of SSA, AOA, GWO, RSA, SCA, and WOA at P_n=90 and I_t=1000



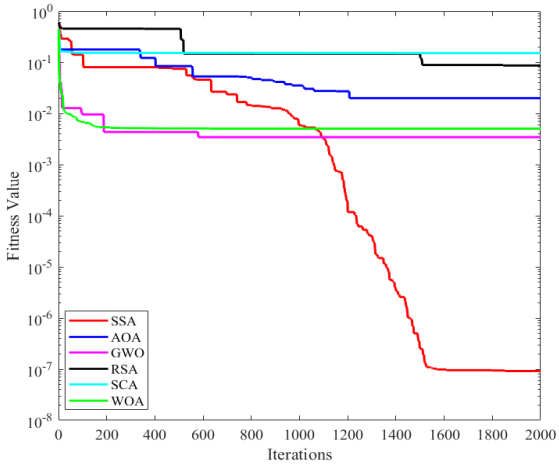
(a) N_e=20dB



(b) N_e=40dB



(c) N_e=60dB



(d) N_e=80dB

Fig. 4 Convergence plot of SSA, AOA, GWO, RSA, SCA,

and WOA at P_n=90 and I_t=2000

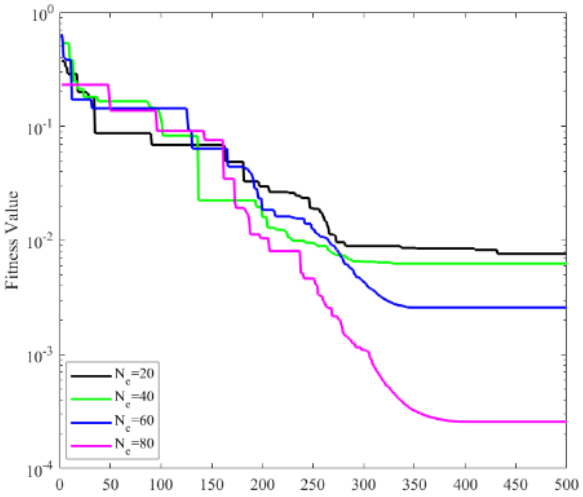
In this study, the harmonic signal is modeled using five dominant harmonic components. This selection is based on the fact that low-order harmonics typically contribute the majority of waveform distortion in practical power systems containing nonlinear loads, power electronic converters, and renewable energy interfaced devices. Moreover, considering five harmonic components provides a representative benchmark that is widely adopted in harmonic parameter estimation studies, enabling a balanced assessment of estimation accuracy while maintaining a manageable optimization search space. Because each harmonic component is characterized by its amplitude and phase angle, the optimization problem has ten decision variables. It is worth noting that the proposed SSA-based estimation framework is not restricted to five harmonic components and can readily be extended to accommodate higher-order harmonics when required by specific power system applications. Moreover, the total variables considered for this problem are 10, out of which 5 represent the phase and 5 represent the amplitude, and it can be expressed as follows.

$$d = [\tau_1, \tau_2, \tau_3, \tau_4, \tau_5, \rho_1, \rho_2, \rho_3, \rho_4, \rho_5] = [1.50,\ 0.50,\ 0.20,\ 0.15,\ 0.10,\ 1.396,\ 1.047,\ 0.785,\ 0.628,\ 0.523] \quad (20)$$

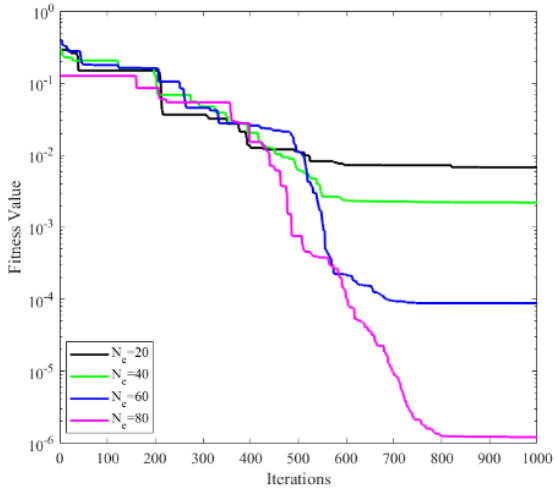
Fig. 2-4 shows the convergence plots SSA, AOA, GWO, RSA, SCA, and WOA. Fig 2 (a-d) shows the convergence plots at I_t = 500. Similarly, Fig 3(a-d) and Fig 4(a-d), show the performance of SSA, AOA, GWO, RSA, SCA, and WOA at I_t = 1000, and I_t = 2000, respectively. It is prominent from Figs. 2-4 that when noise level increases, then fitness value also increases. Moreover, when the iteration increases, the fitness values decrease; however, all variations of SSA achieve the lowest fitness values compared to AOA, GWO, RSA, SCA, and WOA.

Table 1 Pseudocode for salp swarm algorithm

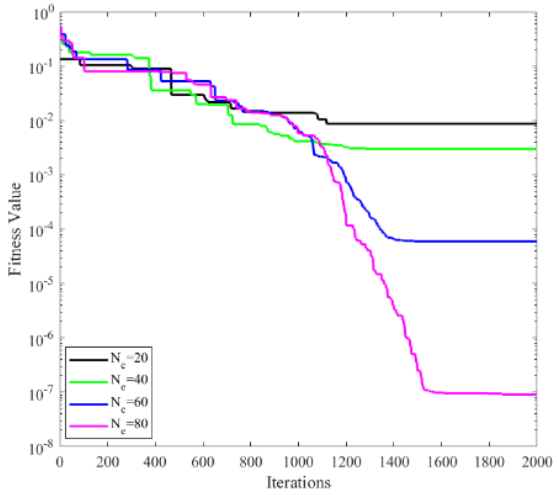
Initialize the salp population x_i *(i = 1, 2, ..., n) considering ub and lb*
while *(end criterion is not met)*
  Calculate the fitness of each search agent (salp)
  Determine the non-dominated salps
  Update the repository considering the obtained non-dominated salps
  if *the repository becomes full*
    Call the repository maintenance procedure to remove one repository resident
    Add the non-dominated salp to the repository
  end
  Choose a source of food from repository: F=SelectFood(repository)
  Update v_1 *by* $v_1 = 2e^{-\left(\frac{4l}{Q}\right)^2}$
  for *each salp (xi)*
    if*(i==1)*
      Update the position of the leading salp by $s_k^1 = \begin{cases} r_k + v_1((pq_k - lq_k)v_2 + lq_k) & v_3 \geq 0 \\ r_k + v_1((pq_k - lq_k)v_2 + lq_k) & v_3 < 0 \end{cases}$
    else
      Update the position of the follower salp by $s_k^m = \frac{1}{2}\left(s_k^m + s_k^{m-1}\right)$
    end
  end
  Amend the salps based on the upper and lower bounds of variables
end
return repository



(a) I_t=500



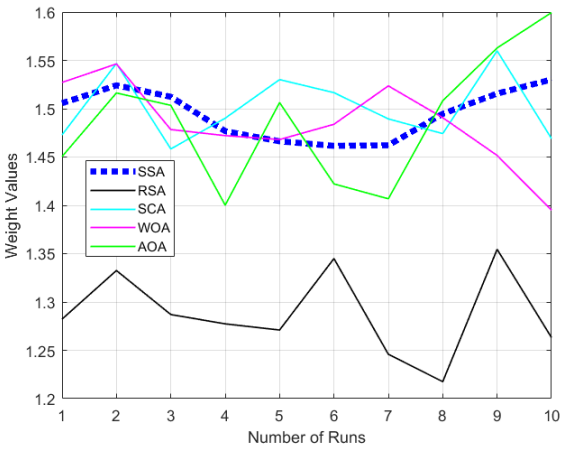
(b) I_t=1000



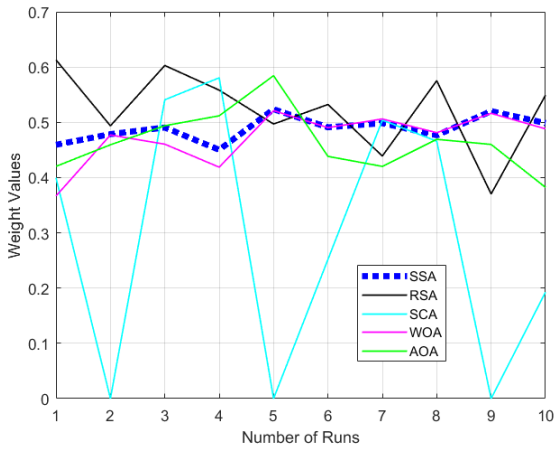
(c) I_t=2000

Fig. 5 Convergence plots of SSA for all noise

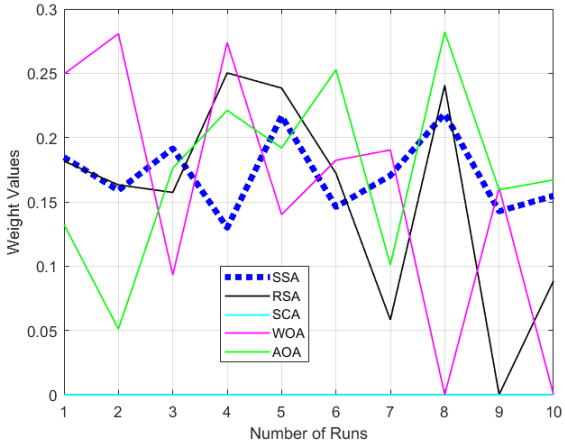
Fig. 5 shows the convergence plots of SSA for all noise levels. Fig 5(a) shows the performance of SSA for Ne = 20 dB, N_e = 40 dB, N_e = 60 dB, and N_e = 80 dB at I_t = 500. Similarly, Figures 5(b) and 5(c) depict performance at It = 1000, and It = 2000, respectively. It can be observed from Fig. 5 (a)- (c) that when noise increases, the fitness value increases. It is also noted that SSA achieves the highest fitness value for N_e = 20dB noise and achieves the lowest fitness for N_e = 80dB noise for all iterations.



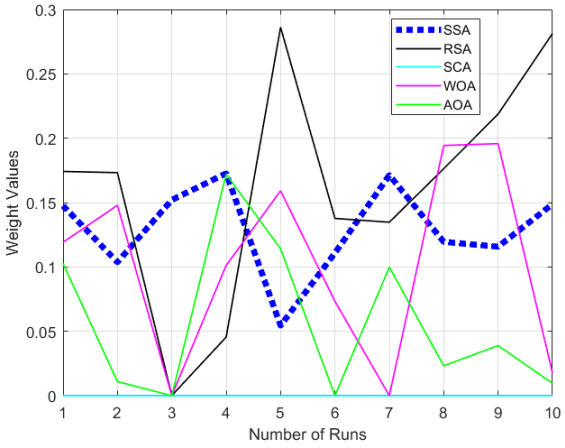
(a) τ_1=1.5



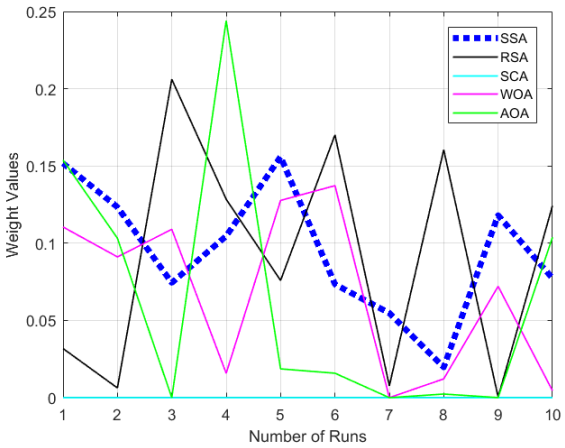
(b) τ_2=0.5



(c) τ_3=0.2

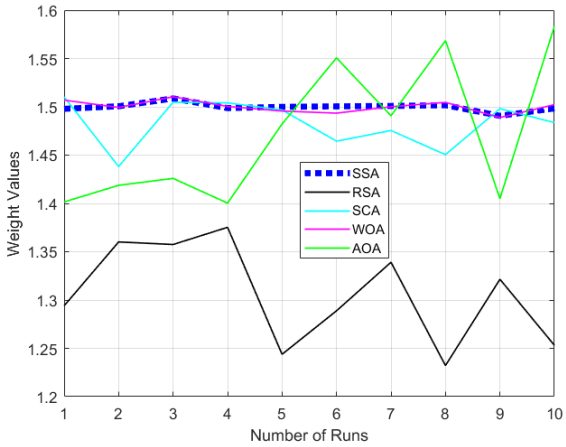


(d) τ_4=0.15

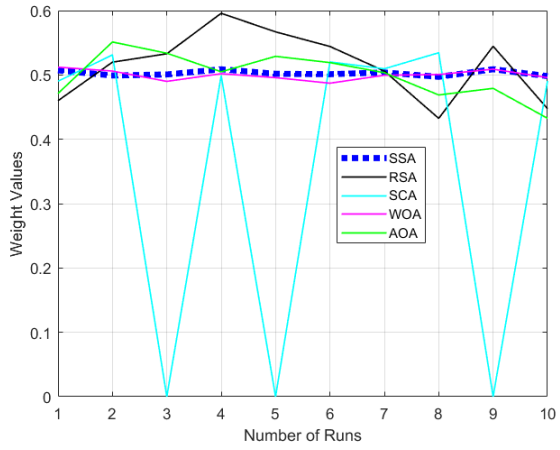


(e) τ_5=0.1

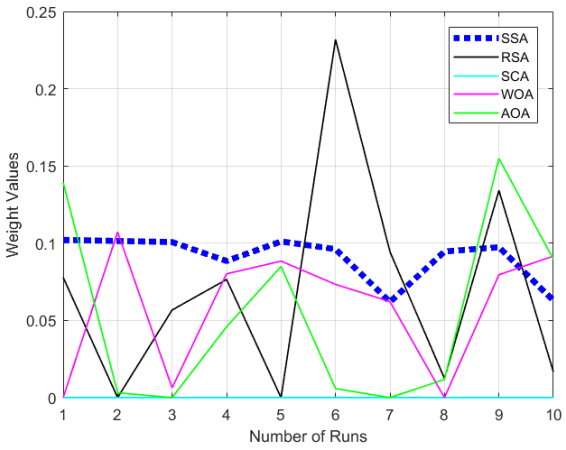
Fig. 6 Comparison of amplitudes w.r. t. N_e = 20dB and I_t = 2000



(a) τ_1=1.5

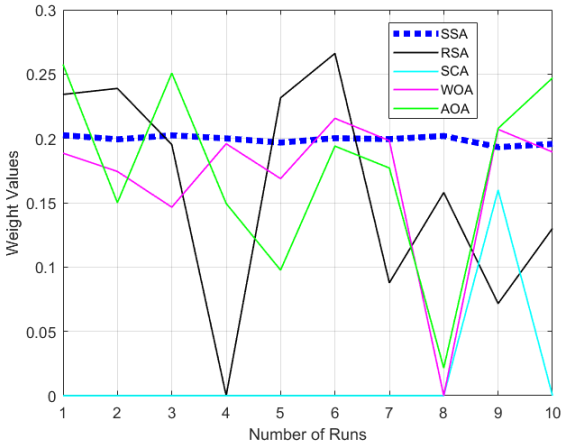


(b) τ_2=0.5

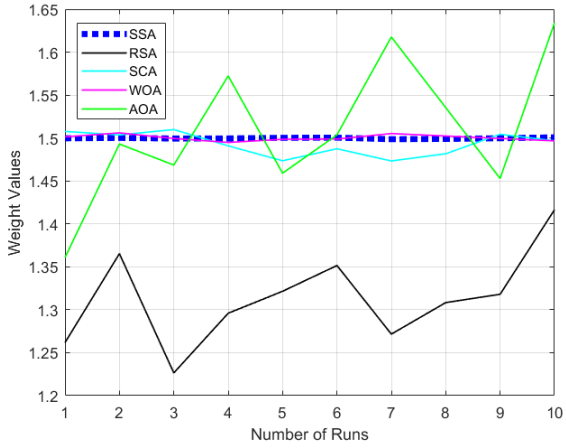


(e) τ_5=0.1

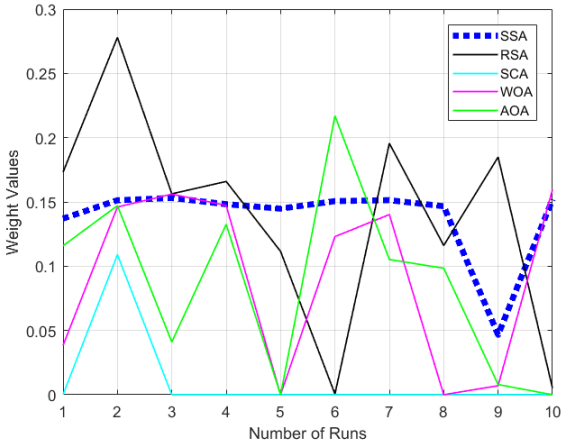
Fig. 7 Comparison of amplitudes w.r. t. N_e = 40dB and I_t = 2000



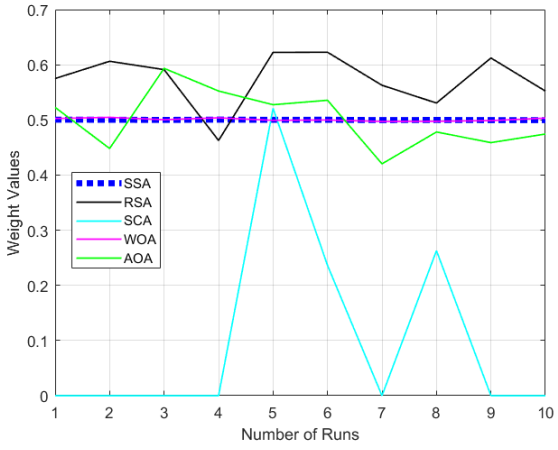
(c) τ_3=0.2



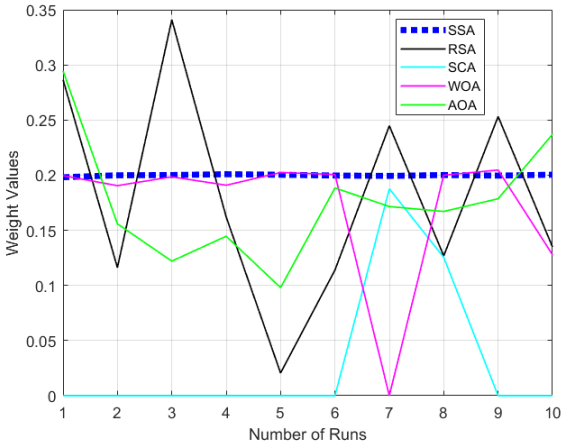
(a) τ_1=1.5



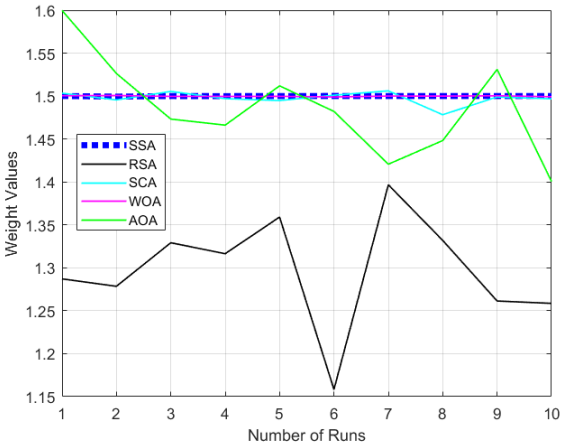
(d) τ_4=0.15



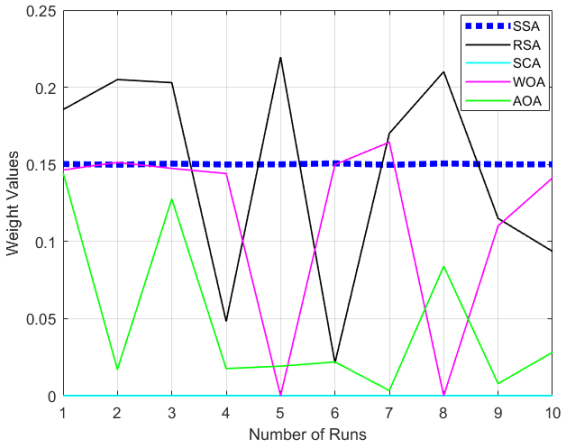
(b) τ_2=0.5



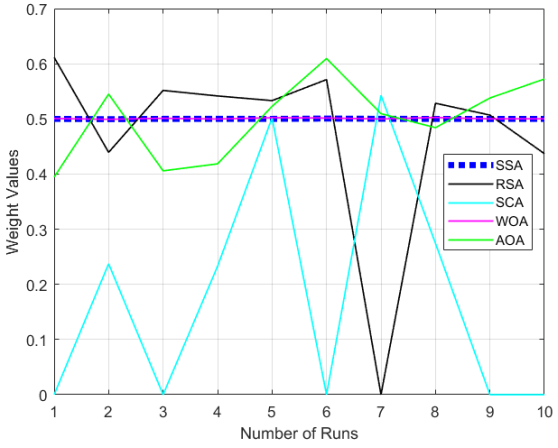
(c) τ_3=0.2



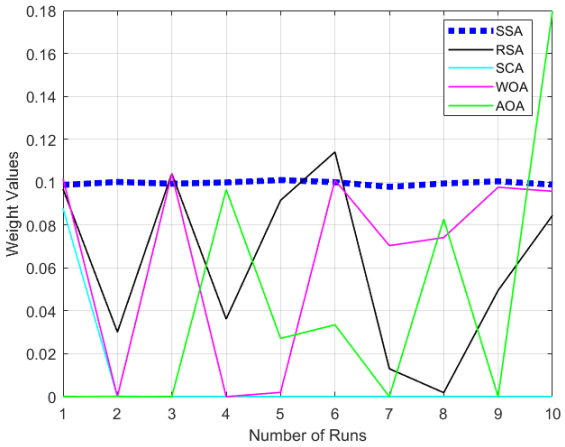
(a) τ_1=1.5



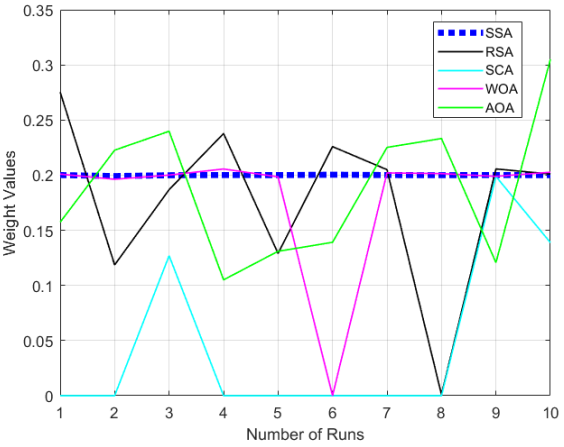
(d) τ_4=0.15



(b) τ_2=0.5

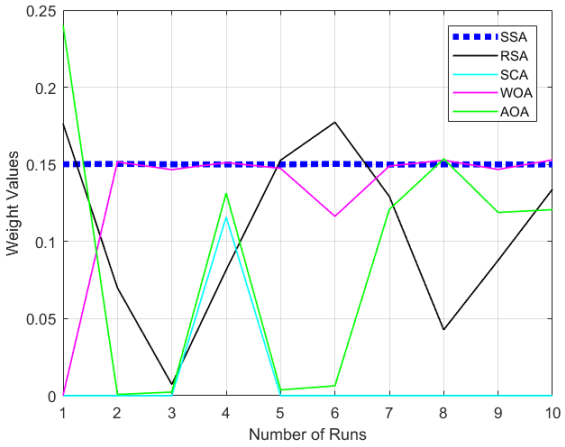


(e) τ_5=0.1

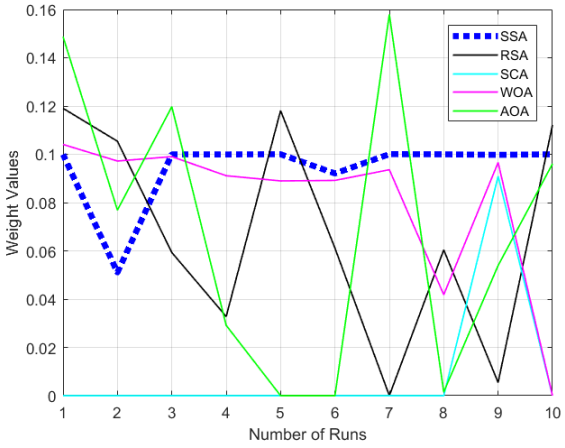


(c) τ_3=0.2

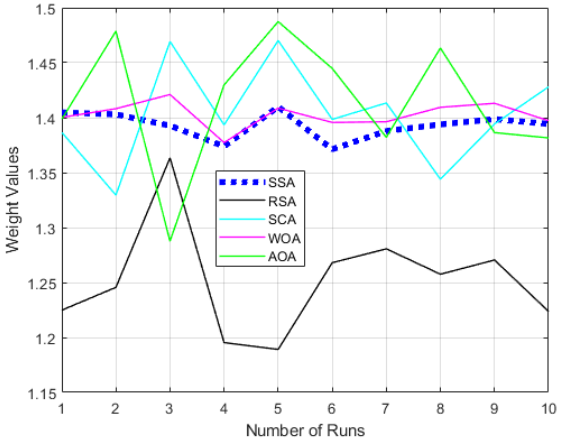
Fig. 8 Comparison of amplitudes w.r. t. N_e = 60dB and I_t = 2000



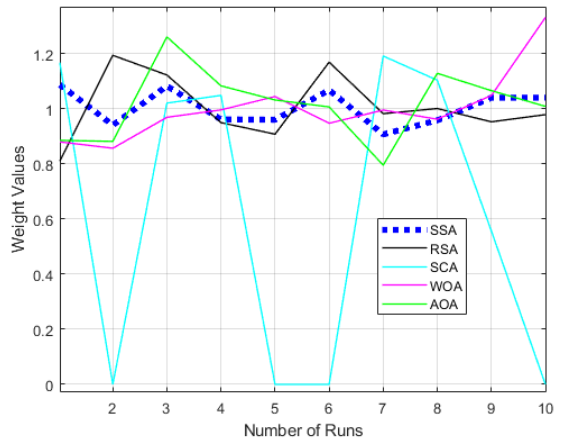
(d) τ_4=0.15



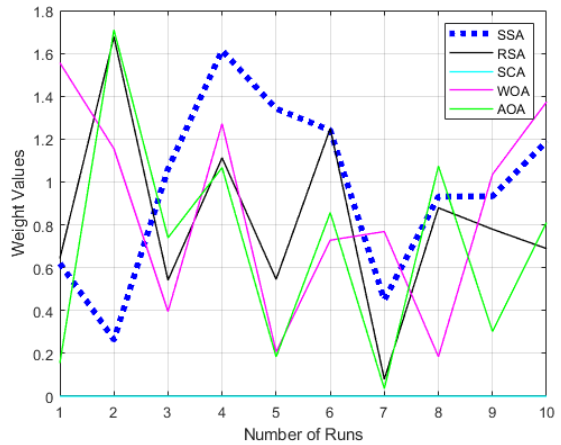
(e) τ_5=0.1



(a) ρ_1=1.396



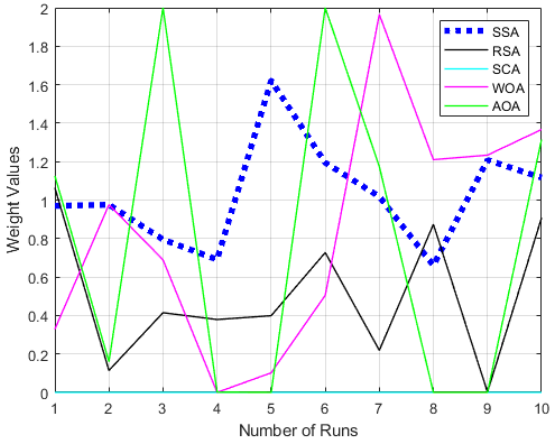
(b) ρ_2=1.047



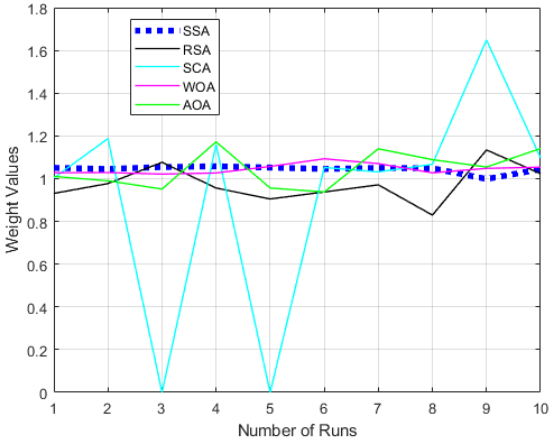
(c) ρ_3=0.785

Fig. 9 Comparison of amplitudes w.r. t. N_e = 80dB and I_t = 2000

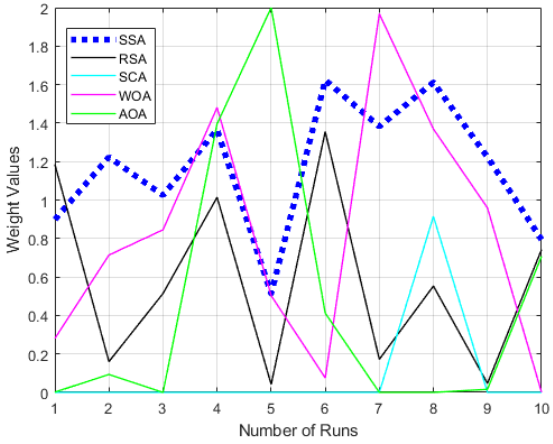
Fig. 6-9 shows the amplitude plots of the harmonic signal for SSA, AOA, RSA, SCA, and WOA for all noise levels. Fig 6 (a-e) shows the weight amplitude plot for Ne = 20dB noise level. Similarly, Fig. 7-9 shows the performance of SSA, AOA, RSA, SCA, and WOA at Ne = 40dB, Ne = 60dB, Ne = 80dB. It can be observed from Fig 6(a-e) that when noise increases, the amplitude value deviates from its true value. It is also noted that SSA achieves the best amplitude value at Ne = 80dB, outperforming the other noise.



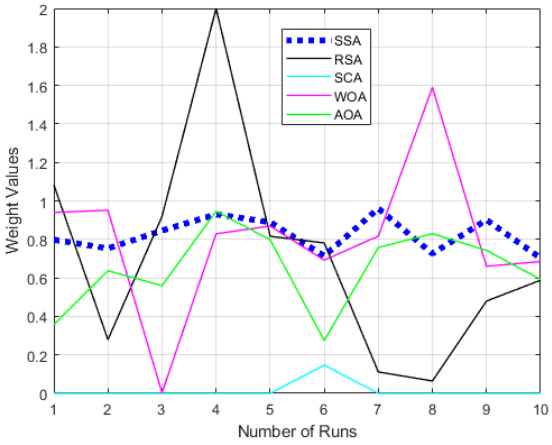
(d) ρ_4=0.628



(b) ρ_2=1.047

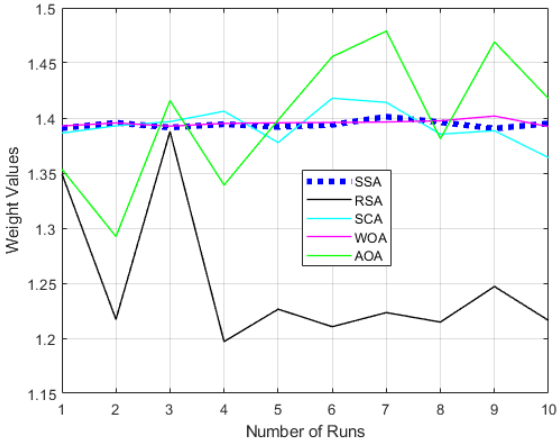


(e) ρ_5=0.523

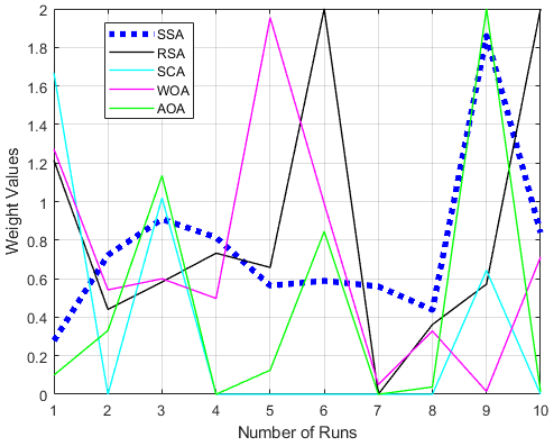


(c) ρ_3=0.785

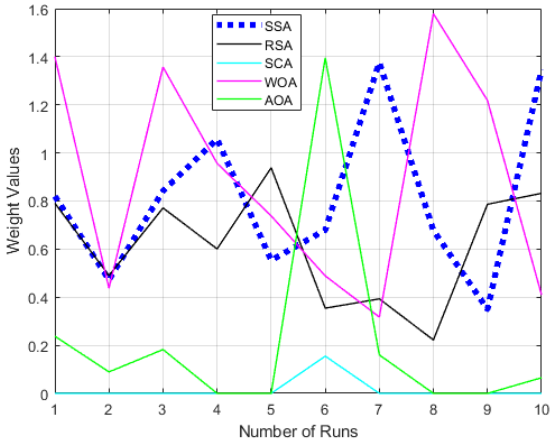
Fig. 10 Comparison of phases w.r. t. N_e = 20dB and I_t = 2000



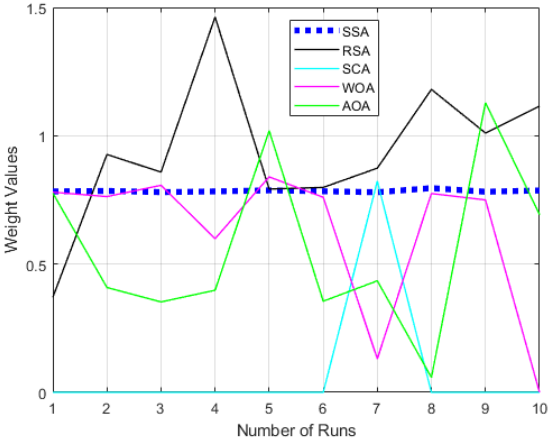
(a) ρ_1=1.396



(d) ρ_4=0.628

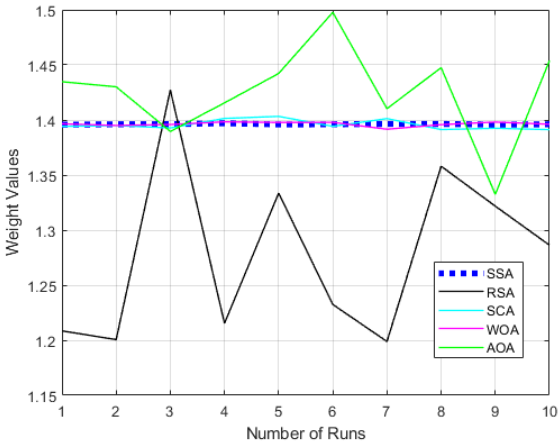


(e) ρ_5=0.523

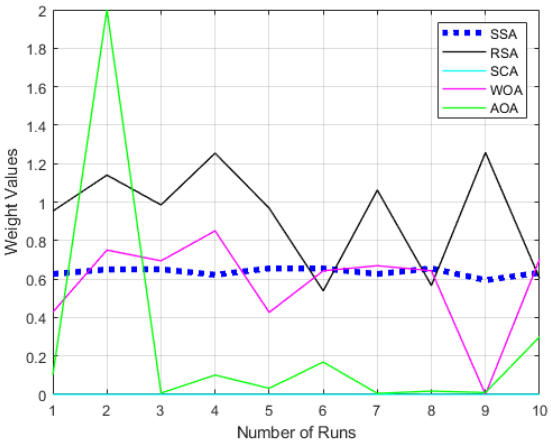


(c) ρ_3=0.785

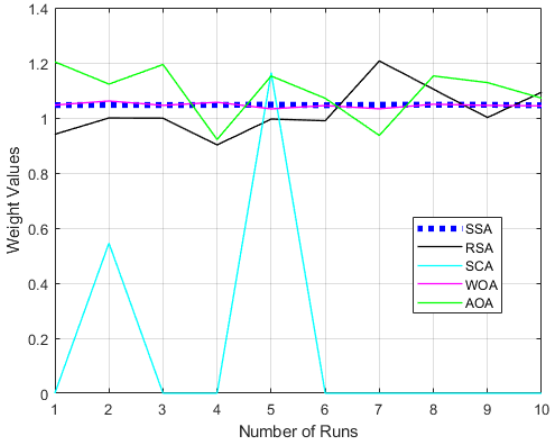
Fig. 11 Comparison of phases w.r. t. N_e = 40dB and I_t = 2000



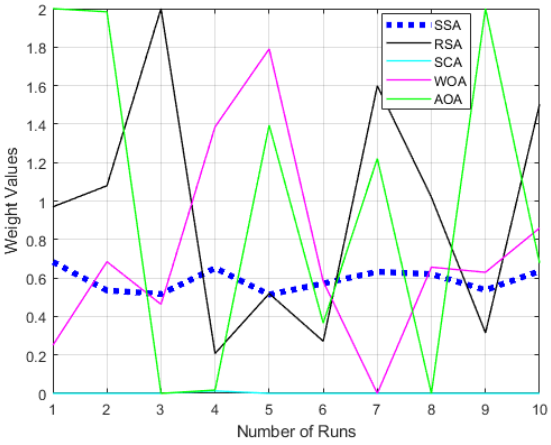
(a) ρ_1=1.396



(d) ρ_4=0.628

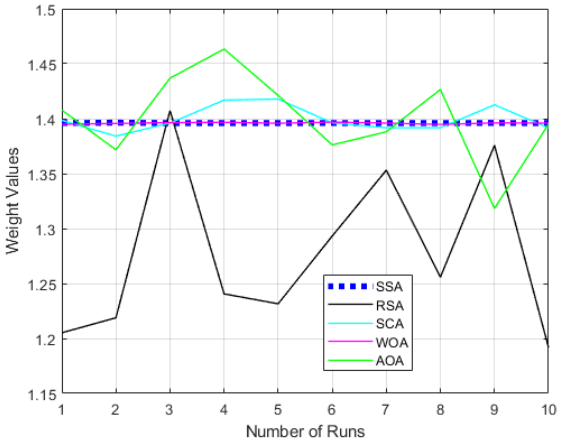


(b) ρ_2=1.047

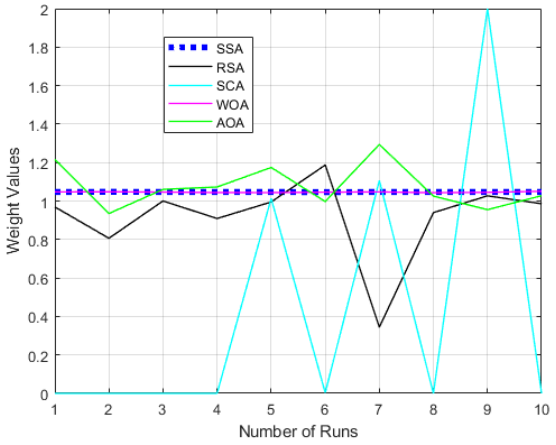


(e) ρ_5=0.523

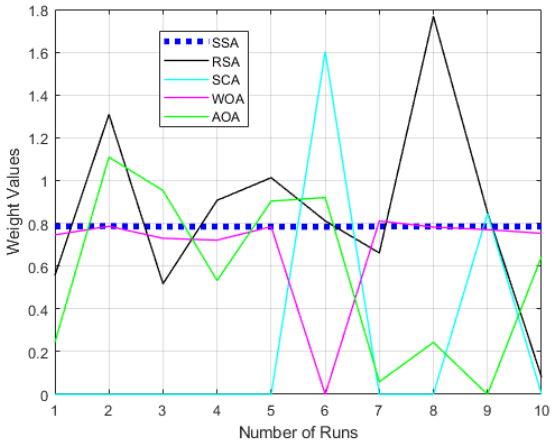
Fig. 12 Comparison of phases w.r. t. N_e = 60dB and I_t = 2000



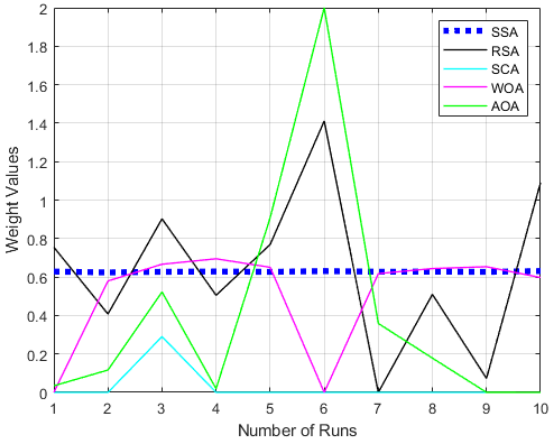
(a) ρ_1=1.396



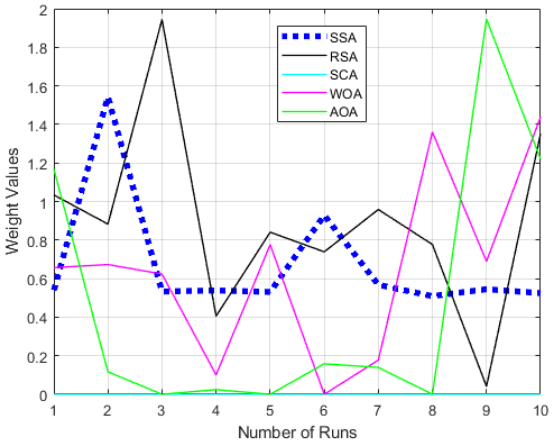
(b) ρ_2=1.047



(c) ρ_3=0.785



(d) ρ_4=0.628



(e) ρ_5=0.523

Fig. 13 Comparison of phases w.r. t. N_e = 80dB and I_t = 2000

Fig. 10-13 show the phase plots of the harmonic signal for SSA, AOA, RSA, SCA, and WOA for all noise levels. Fig 10 (a-e) shows the weight phase plot for a 20 dB noise level. Similarly, Fig. 11-13 show the performance of SSA, AOA, RSA, SCA, and WOA at N_e = 40dB, N_e = 60dB, and N_e = 80dB, respectively. It can be observed from Fig 10(a-e) that when noise increases, the phase value deviates from its true value. It is also noted that SSA achieves the best phase value at N_e = 80dB, and it outperforms the other noise.

Table 2 Analysis of SSA, AOA, GWO, RSA, SCA, and WOA at N_e = 20dB

Method	I_t	P_n	τ_1	τ_2	τ_3	τ_4	τ_5	ρ_1	ρ_2	ρ_3	ρ_4	ρ_5	Best Fitness
SSA	500	30	1.483	0.484	0.194	0.173	0.112	1.388	1.039	0.906	0.574	0.046	6.787e-3
		60	1.492	0.460	0.204	0.126	0.031	1.401	1.042	0.686	0.920	1.644	8.062e-3
		90	1.488	0.483	0.187	0.179	0.072	1.380	1.082	0.850	0.435	0.090	6.975e-3
	1000	30	1.518	0.480	0.209	0.106	0.088	1.393	1.094	0.930	1.031	0.196	8.084e-3
		60	1.516	0.452	0.188	0.181	0.075	1.419	1.044	0.949	0.688	0.685	7.257e-3
		90	1.485	0.503	0.205	0.147	0.099	1.396	1.108	0.857	0.896	0.027	6.743e-3
	2000	30	1.507	0.505	0.221	0.143	0.064	1.419	1.055	0.744	0.803	0.506	6.368e-3
		60	1.473	0.499	0.202	0.124	0.121	1.404	1.041	0.789	0.918	0.204	6.132e-3
		90	1.512	0.490	0.191	0.152	0.074	1.392	1.083	1.060	0.794	1.024	6.433e-3
AOA	500	30	1.397	0.532	0.155	0.177	0.061	1.448	0.946	0.000	0.181	0.013	3.219e-2
		60	1.590	0.556	0.194	0.121	0.000	1.401	0.965	1.055	0.000	0.000	2.610e-2
		90	1.415	0.446	0.083	0.094	0.000	1.366	1.070	0.838	0.002	2.000	2.954e-2
	1000	30	1.619	0.449	0.185	0.133	0.009	1.345	1.082	0.727	0.121	0.145	2.855e-2
		60	1.388	0.456	0.241	0.201	0.012	1.406	1.129	0.294	0.402	0.125	2.673e-2
		90	1.412	0.418	0.294	0.123	0.117	1.378	0.910	0.942	0.000	0.000	2.230e-2
	2000	30	1.416	0.510	0.121	0.041	0.013	1.360	1.047	0.000	0.233	0.179	3.004 e-2
		60	1.563	0.417	0.276	0.135	0.068	1.477	1.045	0.813	0.853	0.000	2.895 e-2
		90	1.562	0.459	0.159	0.038	0.000	1.386	1.066	0.302	0.000	0.016	3.015 e-2
GWO	500	30	1.554	0.455	0.219	0.188	0.075	1.408	1.085	0.546	0.798	0.543	1.272 e-2
		60	1.478	0.524	0.188	0.146	0.0308	1.361	1.028	0.781	0.512	0.382	1.345 e-2
		90	1.528	0.517	0.192	0.173	0.059	1.434	1.019	0.466	0.713	0.290	1.129 e-2
	1000	30	1.521	0.510	0.247	0.114	0.000	1.385	0.893	0.720	0.650	0.000	1.563 e-2
		60	1.464	0.458	0.167	0.103	0.099	1.410	1.055	0.883	0.545	0.387	1.137 e-2
		90	1.503	0.506	0.182	0.117	0.090	1.429	0.930	0.778	0.410	0.000	1.288 e-2
	2000	30	1.489	0.553	0.147	0.135	0.016	1.407	0.958	0.875	0.434	0.083	1.471 e-2
		60	1.522	0.455	0.197	0.131	0.075	1.417	1.173	0.619	0.548	0.118	1.098 e-2
		90	1.486	0.464	0.173	0.122	0.093	1.388	1.055	0.947	0.748	0.149	1.116e-2
RSA	500	30	1.390	0.608	0.305	0.185	0.132	1.401	1.065	0.790	0.811	1.272	3.316e-2
		60	1.414	0.485	0.273	0.024	0.017	1.257	0.911	1.011	1.165	0.000	4.933e-2
		90	1.436	0.451	0.091	0.146	0.008	1.264	1.094	0.646	0.664	2.000	4.255e-2
	1000	30	1.365	0.408	0.083	0.000	0.002	1.226	1.020	0.013	0.125	1.218	7.520e-2
		60	1.351	0.538	0.179	0.061	0.002	1.216	1.021	1.072	0.562	1.535	5.844e-2
		90	1.371	0.586	0.205	0.230	0.007	1.299	1.000	1.112	0.868	1.059	3.845e-2
	2000	30	1.480	0.549	0.228	0.105	0.020	1.273	0.979	1.058	0.987	1.998	3.458e-2
		60	1.419	0.563	0.217	0.028	0.073	1.353	0.980	1.027	0.791	0.367	2.411e-2
		90	1.344	0.532	0.172	0.137	0.170	1.268	1.170	1.249	0.727	1.355	4.491e-2
SCA	500	30	1.479	0.449	0.000	0.000	0.000	1.312	1.210	0.000	0.000	0.000	4.517e-2
		60	1.516	0.548	0.000	0.000	0.000	1.396	1.051	0.000	0.000	0.781	4.155e-2
		90	1.440	0.467	0.000	0.113	0.000	1.351	0.883	0.442	1.311	0.000	4.081e-2
	1000	30	1.536	0.614	0.000	0.000	0.000	1.370	0.873	0.000	0.000	0.815	5.056e-2
		60	1.555	0.478	0.107	0.001	0.000	1.419	0.834	1.249	0.587	0.000	3.519e-2
		90	1.512	0.546	0.000	0.000	0.000	1.388	0.964	0.000	0.022	0.057	3.943e-2
	2000	30	1.467	0.480	0.000	0.000	0.000	1.341	1.145	0.000	0.000	0.000	4.183e-2
		60	1.526	0.508	0.000	0.146	0.000	1.450	1.159	0.000	0.000	0.000	3.563e-2
		90	1.489	0.503	0.000	0.000	0.000	1.413	1.192	0.000	0.000	0.000	3.757e-2
WOA	500	30	1.424	0.505	0.290	0.167	0.036	1.439	1.013	1.096	0.452	0.141	1.553e-2
		60	1.473	0.554	0.122	0.131	0.131	1.386	1.002	0.892	0.119	0.992	1.197e-2
		90	1.444	0.223	0.269	0.088	0.112	1.398	0.049	0.013	1.420	1.106	1.129e-2
	1000	30	1.486	0.488	0.151	0.190	0.096	1.412	1.085	1.115	1.304	0.000	1.269e-2
		60	1.475	0.442	0.195	0.159	0.101	1.409	0.884	1.231	0.723	0.814	1.165e-2
		90	1.512	0.396	0.196	0.189	0.093	1.414	1.062	0.867	1.136	0.501	1.139e-2
	2000	30	1.465	0.439	0.202	0.097	0.137	1.450	0.965	1.097	1.562	0.727	1.670e-2
		60	1.500	0.459	0.179	0.128	0.140	1.407	0.943	0.979	0.621	0.051	9.348e-3
		90	1.483	0.490	0.182	0.073	0.137	1.395	0.948	0.728	0.504	0.075	8.356e-3
Actual			1.500	0.500	0.200	0.150	0.100	1.396	1.047	0.785	0.628	0.523	

Table 3: Analysis of SSA, AOA, GWO, RSA, SCA, and WOA at N_e = 40dB

Method	I_t	P_n	τ_1	τ_2	τ_3	τ_4	τ_5	ρ_1	ρ_2	ρ_3	ρ_4	ρ_5	Best Fitness
SSA	500	30	1.498	0.498	0.198	0.149	0.099	1.396	1.057	0.684	0.684	0.447	2.642e-04
		60	1.494	0.502	0.199	0.148	0.103	1.400	1.054	0.685	0.557	0.610	2.916e-04
		90	1.497	0.501	0.198	0.144	0.107	1.396	1.040	0.874	0.587	0.624	2.576e-04
	1000	30	1.494	0.504	0.203	0.142	0.098	1.403	1.029	0.691	0.714	0.668	4.328e-04
		60	1.498	0.501	0.201	0.148	0.098	1.397	1.063	0.795	0.514	0.317	3.353e-04
		90	1.496	0.499	0.200	0.144	0.091	1.393	1.040	0.776	0.658	0.772	3.072e-04
	2000	30	1.497	0.496	0.198	0.146	0.092	1.396	1.048	0.783	0.537	0.710	2.588e-04
		60	1.502	0.502	0.199	0.147	0.099	1.395	1.053	0.740	0.837	0.324	6.239e-04
		90	1.500	0.499	0.199	0.151	0.101	1.395	1.045	0.752	0.722	0.472	1.384e-04
AOA	500	30	1.510	0.528	0.145	0.189	0.000	1.315	1.041	0.278	0.000	0.090	2.338e-02
		60	1.553	0.424	0.100	0.011	0.141	1.416	1.112	0.156	0.196	0.026	2.589e-02
		90	1.503	0.453	0.171	0.016	0.000	1.351	0.914	0.576	0.000	2.000	2.139e-02
	1000	30	1.585	0.456	0.117	0.085	0.000	1.412	0.931	0.980	1.168	0.089	1.950e-02
		60	1.600	0.501	0.221	0.238	0.013	1.424	0.948	0.425	0.369	2.000	2.058e-02
		90	1.553	0.542	0.205	0.001	0.106	1.368	1.201	0.652	0.002	0.173	1.936e-02
	2000	30	1.535	0.483	0.102	0.233	0.161	1.388	0.983	0.109	0.350	0.618	1.763e-02
		60	1.536	0.436	0.162	0.036	0.152	1.396	1.098	0.033	0.155	0.001	2.319e-02
		90	1.490	0.503	0.177	0.105	0.000	1.478	1.139	0.758	0.000	0.160	1.774e-02
GWO	500	30	1.508	0.531	0.184	0.110	0.008	1.424	0.959	0.581	0.494	0.511	8.623e-03
		60	1.464	0.498	0.231	0.109	0.077	1.415	0.942	0.619	0.210	0.364	6.117e-03
		90	1.492	0.513	0.175	0.131	0.105	1.388	1.066	0.729	0.501	0.142	1.793e-03
	1000	30	1.494	0.490	0.195	0.111	0.034	1.446	1.058	0.755	0.495	0.437	6.066e-03
		60	1.484	0.468	0.160	0.151	0.093	1.366	0.995	1.037	0.841	0.805	4.799e-03
		90	1.503	0.529	0.235	0.106	0.076	1.384	1.027	0.731	0.610	0.008	3.663e-03
	2000	30	1.499	0.510	0.153	0.164	0.111	1.407	1.138	0.982	0.441	0.066	4.804e-03
		60	1.487	0.450	0.224	0.155	0.093	1.391	1.097	0.724	0.184	0.048	5.213e-03
		90	1.478	0.507	0.222	0.125	0.072	1.420	1.063	0.761	0.728	0.542	2.079e-03
RSA	500	30	1.455	0.538	0.139	0.103	0.249	1.245	1.030	1.132	0.494	1.123	4.716e-02
		60	1.309	0.457	0.058	0.063	0.001	1.414	1.014	0.255	0.142	0.457	4.129e-02
		90	1.459	0.545	0.125	0.059	0.025	1.346	0.982	0.027	0.115	0.344	2.330e-02
	1000	30	1.247	0.519	0.351	0.210	0.189	1.292	1.131	0.837	0.484	0.931	6.241e-02
		60	1.439	0.531	0.000	0.024	0.120	1.318	0.937	1.311	1.911	0.346	4.125e-02
		90	1.432	0.470	0.260	0.020	0.040	1.366	0.894	0.760	0.555	1.497	2.049e-02
	2000	30	1.262	0.563	0.127	0.010	0.001	1.291	0.943	0.603	1.316	0.344	5.971e-02
		60	1.409	0.561	0.089	0.026	0.137	1.321	1.010	0.402	0.057	0.636	2.833e-02
		90	1.357	0.532	0.195	0.156	0.056	1.387	1.076	0.919	0.583	0.771	1.235e-02
SCA	500	30	1.466	0.489	0.000	0.000	0.000	1.433	0.948	0.000	0.000	0.000	3.915e-02
		60	1.405	0.673	0.171	0.155	0.091	1.452	0.965	0.979	0.998	0.476	2.702e-02
		90	1.555	0.458	0.181	0.000	0.000	1.399	1.031	0.000	0.000	0.000	2.966e-02
	1000	30	1.449	0.475	0.000	0.000	0.003	1.364	1.040	0.000	0.000	1.560	3.927e-02
		60	1.442	0.495	0.237	0.000	0.000	1.421	1.124	0.971	0.048	0.002	2.064e-02
		90	1.473	0.512	0.000	0.095	0.000	1.447	1.049	1.621	0.000	0.972	3.269e-02
	2000	30	1.505	0.482	0.000	0.000	0.000	1.372	1.030	0.000	0.000	0.000	3.702e-02
		60	1.538	0.521	0.000	0.000	0.000	1.412	1.037	0.000	0.000	0.000	3.719e-02
		90	1.438	0.531	0.000	0.108	0.000	1.392	1.187	0.000	0.000	0.000	3.363e-02
WOA	500	30	1.496	0.487	0.204	0.171	0.041	1.399	1.086	0.518	0.748	0.048	3.996e-03
		60	1.495	0.506	0.197	0.115	0.127	1.400	1.020	0.808	0.497	1.045	2.741e-03
		90	1.491	0.500	0.186	0.147	0.133	1.400	1.040	0.904	0.570	0.628	9.641e-04
	1000	30	1.505	0.484	0.221	0.144	0.115	1.395	1.011	0.913	0.777	0.011	2.440e-03
		60	1.508	0.494	0.185	0.128	0.114	1.392	1.055	0.861	0.717	0.465	6.377e-04
		90	1.494	0.509	0.177	0.143	0.085	1.396	1.077	0.741	0.676	0.260	7.988e-04
	2000	30	1.499	0.501	0.185	0.161	0.078	1.401	1.019	1.033	0.526	0.292	1.718e-03
		60	1.495	0.509	0.199	0.119	0.096	1.397	1.060	0.714	0.716	0.925	1.318e-03
		90	1.502	0.495	0.189	0.159	0.091	1.392	1.053	0.684	0.712	0.409	4.337e-04
Actual			1.500	0.500	0.200	0.150	0.100	1.396	1.047	0.785	0.628	0.523	

Table 4 Analysis of SSA, AOA, GWO, RSA, SCA, and WOA at N_e = 60dB

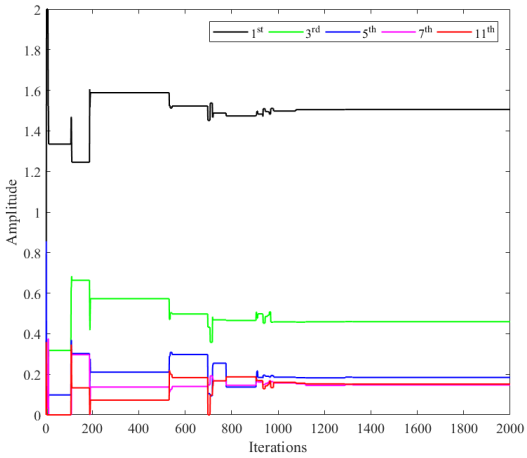
Method	I_t	P_n	τ_1	τ_2	τ_3	τ_4	τ_5	ρ_1	ρ_2	ρ_3	ρ_4	ρ_5	Best Fitness
SSA	500	30	1.499	0.500	0.198	0.149	0.095	1.396	1.048	0.851	0.626	0.782	4.051e-04
		60	1.499	0.500	0.199	0.150	0.100	1.395	1.046	0.768	0.699	0.468	7.432e-05
		90	1.500	0.500	0.200	0.150	0.099	1.395	1.045	0.810	0.664	0.459	4.473e-05
	1000	30	1.499	0.500	0.199	0.150	0.099	1.396	1.047	0.821	0.634	0.595	4.860e-05
		60	1.499	0.499	0.199	0.149	0.100	1.395	1.047	0.793	0.639	0.528	2.882e-06
		90	1.500	0.499	0.200	0.150	0.100	1.395	1.045	0.790	0.654	0.551	1.164e-05
	2000	30	1.500	0.499	0.200	0.150	0.099	1.396	1.046	0.771	0.635	0.471	1.557e-05
		60	1.499	0.500	0.199	0.150	0.099	1.395	1.047	0.783	0.647	0.485	1.034e-05
		90	1.500	0.500	0.199	0.149	0.100	1.396	1.047	0.785	0.649	0.535	5.072e-06
AOA	500	30	1.571	0.476	0.117	0.003	0.126	1.468	0.951	0.031	2.000	0.217	3.178e-02
		60	1.473	0.497	0.190	0.153	0.000	1.329	0.929	0.101	0.000	0.119	2.492e-02
		90	1.410	0.477	0.233	0.010	0.001	1.442	1.111	1.021	2.000	0.000	2.484e-02
	1000	30	1.489	0.601	0.179	0.171	0.141	1.299	0.998	0.331	0.318	0.262	2.270e-02
		60	1.527	0.502	0.247	0.073	0.000	1.439	1.116	0.636	0.003	0.216	1.482e-02
		90	1.417	0.478	0.245	0.155	0.000	1.476	0.922	0.534	0.184	0.000	2.216e-02
	2000	30	1.395	0.425	0.156	0.172	0.060	1.431	0.785	0.942	0.405	0.097	2.031e-02
		60	1.594	0.492	0.113	0.156	0.011	1.366	1.154	0.679	0.000	0.021	1.938e-02
		90	1.535	0.478	0.167	0.083	0.082	1.447	1.152	0.058	0.017	0.000	1.993e-02
GWO	500	30	1.495	0.542	0.239	0.147	0.071	1.415	0.985	0.524	0.411	0.077	5.876e-03
		60	1.511	0.478	0.185	0.127	0.068	1.404	0.968	0.665	0.570	0.014	3.136e-03
		90	1.521	0.460	0.158	0.159	0.103	1.406	1.089	0.710	0.723	0.538	2.456e-03
	1000	30	1.510	0.567	0.233	0.175	0.122	1.388	1.131	0.789	0.506	0.448	4.809e-03
		60	1.483	0.484	0.138	0.114	0.089	1.404	1.054	0.666	0.701	0.447	3.157e-03
		90	1.530	0.457	0.201	0.163	0.095	1.403	1.060	0.961	0.560	0.334	2.403e-03
	2000	30	1.453	0.463	0.211	0.144	0.071	1.386	1.012	0.983	0.328	0.019	5.150e-03
		60	1.544	0.512	0.241	0.155	0.084	1.390	1.125	0.872	0.567	0.877	3.669e-03
		90	1.480	0.503	0.216	0.164	0.103	1.385	1.122	1.018	0.464	0.683	2.933e-03
RSA	500	30	1.391	0.558	0.267	0.280	0.068	1.212	0.990	0.831	0.993	0.728	5.717e-02
		60	1.339	0.497	0.160	0.032	0.024	1.327	1.242	1.180	1.125	1.633	3.728e-02
		90	1.457	0.544	0.150	0.167	0.088	1.314	1.011	1.109	0.656	0.025	1.341e-02
	1000	30	1.389	0.499	0.075	0.000	0.000	1.334	1.013	0.000	0.927	1.737	3.848e-02
		60	1.312	0.449	0.209	0.207	0.080	1.272	1.040	0.711	0.236	0.920	3.883e-02
		90	1.309	0.573	0.261	0.221	0.092	1.301	1.185	0.574	0.585	0.531	3.802e-02
	2000	30	1.389	0.519	0.133	0.078	0.001	1.348	0.885	0.392	0.395	2.000	2.408e-02
		60	1.326	0.475	0.186	0.009	0.212	1.218	0.905	0.356	0.005	0.306	6.919e-02
		90	1.416	0.552	0.134	0.093	0.084	1.286	1.093	1.115	0.603	1.502	2.689e-02
SCA	500	30	1.509	0.557	0.000	0.000	0.000	1.436	1.102	0.000	0.989	0.000	4.016e-02
		60	1.470	0.493	0.000	0.165	0.000	1.345	0.920	0.000	0.000	0.010	3.517e-02
		90	1.481	0.516	0.057	0.082	0.000	1.391	1.091	0.209	0.000	0.000	2.227e-02
	1000	30	1.525	0.229	0.000	0.000	0.000	1.389	0.000	0.000	0.000	1.056	1.305e-01
		60	1.484	0.530	0.155	0.000	0.000	1.426	1.131	0.000	0.000	0.000	2.896e-02
		90	1.500	0.471	0.000	0.000	0.000	1.383	1.035	0.000	0.000	0.000	3.677e-02
	2000	30	1.536	0.506	0.000	0.119	0.000	1.377	0.998	0.000	0.000	0.000	3.030e-02
		60	1.501	0.497	0.000	0.000	0.097	1.389	1.147	0.000	0.000	0.000	3.385e-02
		90	1.473	0.520	0.000	0.000	0.000	1.403	1.164	0.000	0.000	0.000	3.866e-02
WOA	500	30	1.499	0.492	0.137	0.160	0.093	1.392	1.058	1.111	0.707	0.455	3.565e-03
		60	1.500	0.499	0.189	0.152	0.106	1.395	1.047	0.833	0.667	0.565	1.477e-04
		90	1.497	0.499	0.209	0.151	0.076	1.395	1.052	0.718	0.782	0.536	6.826e-04
	1000	30	1.498	0.498	0.208	0.144	0.102	1.395	1.053	0.805	0.237	0.709	1.852e-03
		60	1.503	0.499	0.199	0.163	0.078	1.394	1.046	0.756	0.694	0.280	6.091e-04
		90	1.500	0.496	0.194	0.151	0.095	1.394	1.043	0.875	0.661	0.649	2.730e-04
	2000	30	1.500	0.501	0.202	0.124	0.081	1.397	1.033	0.624	0.803	1.077	2.531e-03
		60	1.498	0.501	0.194	0.145	0.093	1.396	1.050	0.803	0.603	0.499	6.031e-05
		90	1.498	0.499	0.2006	0.149	0.100	1.397	1.044	0.760	0.642	0.581	3.403e-05
Actual			1.500	0.500	0.200	0.150	0.100	1.396	1.047	0.785	0.628	0.523	

Table 5 Analysis of SSA, AOA, GWO, RSA, SCA, and WOA at N_e = 80dB

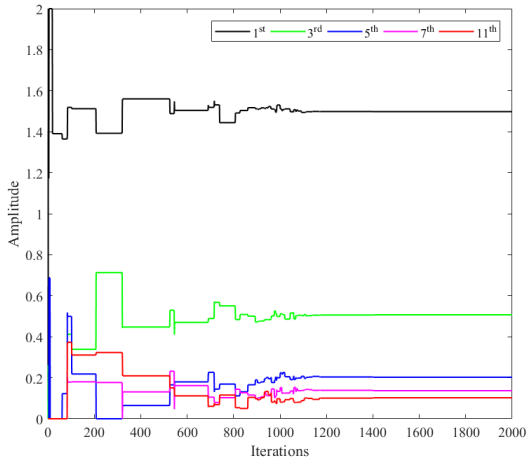
Method	I_t	P_n	τ_1	τ_2	τ_3	τ_4	τ_5	ρ_1	ρ_2	ρ_3	ρ_4	ρ_5	Best Fitness
SSA	500	30	1.500	0.500	0.199	0.149	0.098	1.395	1.047	0.789	0.700	0.713	2.372e-04
		60	1.500	0.500	0.199	0.150	0.099	1.395	1.046	0.798	0.615	0.673	1.176e-04
		90	1.499	0.499	0.199	0.149	0.099	1.395	1.047	0.775	0.677	0.627	8.307e-05
	1000	30	1.500	0.500	0.199	0.150	0.099	1.395	1.047	0.787	0.633	0.544	2.756e-06
		60	1.499	0.499	0.200	0.150	0.099	1.396	1.047	0.785	0.635	0.519	5.730e-07
		90	1.500	0.500	0.200	0.149	0.100	1.396	1.047	0.786	0.631	0.514	5.102e-07
	2000	30	1.499	0.500	0.199	0.150	0.099	1.395	1.047	0.787	0.625	0.535	8.648e-07
		60	1.499	0.499	0.200	0.150	0.099	1.396	1.046	0.784	0.632	0.529	4.805e-07
		90	1.500	0.500	0.200	0.149	0.100	1.395	1.046	0.784	0.630	0.524	9.182e-08
AOA	500	30	1.491	0.587	0.220	0.063	0.000	1.338	1.063	0.316	0.005	2.000	2.299e-02
		60	1.379	0.559	0.154	0.003	0.112	1.424	1.054	0.705	0.006	0.547	2.200e-02
		90	1.521	0.416	0.214	0.001	0.000	1.369	1.091	0.930	0.090	0.016	2.132e-02
	1000	30	1.597	0.551	0.250	0.118	0.000	1.433	0.930	0.442	0.000	0.007	2.264e-02
		60	1.442	0.458	0.244	0.178	0.000	1.378	0.967	1.016	0.382	0.026	1.211e-02
		90	1.592	0.562	0.175	0.151	0.000	1.427	1.211	0.544	0.289	0.024	1.875e-02
	2000	30	1.536	0.467	0.155	0.006	0.000	1.408	1.036	0.598	2.000	2.000	1.897e-02
		60	1.596	0.480	0.233	0.129	0.000	1.414	1.082	0.534	0.000	2.000	1.634e-02
		90	1.448	0.484	0.233	0.153	0.001	1.426	1.025	0.243	0.178	0.000	1.693e-02
GWO	500	30	1.520	0.450	0.211	0.174	0.082	1.417	1.010	0.484	0.394	1.084	6.541e-03
		60	1.479	0.484	0.239	0.139	0.136	1.415	0.987	0.642	0.522	0.388	3.385e-03
		90	1.496	0.494	0.167	0.161	0.056	1.388	1.017	0.679	0.558	0.621	1.981e-03
	1000	30	1.479	0.481	0.191	0.144	0.061	1.402	0.952	0.672	0.071	0.083	6.401e-03
		60	1.513	0.483	0.182	0.131	0.066	1.399	1.058	0.906	0.430	0.294	1.986e-03
		90	1.516	0.530	0.167	0.128	0.113	1.405	1.138	0.691	0.459	0.578	3.093e-03
	2000	30	1.527	0.536	0.186	0.206	0.049	1.386	1.088	0.899	0.777	0.001	5.582e-03
		60	1.518	0.468	0.184	0.169	0.048	1.406	1.035	0.778	0.593	0.190	2.711e-03
		90	1.482	0.522	0.251	0.143	0.080	1.409	1.035	0.564	0.611	0.452	3.439e-03
RSA	500	30	1.413	0.461	0.262	0.147	0.103	1.228	0.922	0.308	0.455	1.179	4.630e-02
		60	1.343	0.519	0.151	0.000	0.032	1.324	1.407	0.606	0.147	0.509	4.932e-02
		90	1.268	0.586	0.226	0.056	0.101	1.286	0.850	0.647	1.048	0.554	5.339e-02
	1000	30	1.354	0.406	0.337	0.262	0.054	1.418	1.115	1.152	0.918	0.713	3.913e-02
		60	1.308	0.577	0.322	0.191	0.081	1.327	0.860	0.840	0.676	0.909	4.025e-02
		90	1.304	0.513	0.206	0.000	0.023	1.387	1.001	0.947	1.832	0.980	3.447e-02
	2000	30	1.247	0.458	0.126	0.277	0.130	1.425	1.052	0.751	0.723	0.852	4.587e-02
		60	1.333	0.456	0.306	0.165	0.054	1.357	0.999	0.629	0.982	1.761	2.930e-02
		90	1.329	0.551	0.186	0.007	0.059	1.407	1.000	0.517	0.902	1.944	3.386e-02
SCA	500	30	1.480	0.499	0.000	0.000	0.000	1.423	1.042	0.000	0.000	0.000	3.729e-02
		60	1.413	0.518	0.304	0.000	0.000	1.372	1.015	0.667	0.000	0.000	2.674e-02
		90	1.445	0.456	0.146	0.000	0.004	1.421	1.080	0.000	0.000	0.000	2.916e-02
	1000	30	1.478	0.571	0.166	0.000	0.000	1.423	0.981	0.207	0.000	0.000	2.647e-02
		60	1.498	0.531	0.000	0.000	0.000	1.375	1.074	0.000	0.526	0.000	3.730e-02
		90	1.515	0.527	0.146	0.000	0.000	1.389	1.118	0.000	0.000	0.000	2.748e-02
	2000	30	1.474	0.490	0.000	0.138	0.000	1.420	1.062	0.000	0.738	0.029	2.627e-02
		60	1.464	0.491	0.156	0.000	0.000	1.404	1.087	1.012	0.000	0.000	1.894e-02
		90	1.494	0.501	0.000	0.000	0.000	1.417	1.013	0.000	0.000	0.000	3.693e-02
WOA	500	30	1.500	0.505	0.211	0.183	0.138	1.395	0.985	0.406	0.282	0.595	6.471e-03
		60	1.500	0.491	0.193	0.157	0.119	1.394	1.042	0.777	0.793	0.747	8.936e-04
		90	1.499	0.505	0.208	0.137	0.097	1.396	1.029	0.830	0.396	0.517	7.650e-04
	1000	30	1.498	0.510	0.199	0.137	0.104	1.396	1.047	0.574	0.640	0.195	1.573e-03
		60	1.500	0.500	0.195	0.158	0.084	1.395	1.044	0.786	0.657	0.664	2.546e-04
		90	1.500	0.502	0.198	0.152	0.099	1.395	1.044	0.708	0.728	0.544	2.403e-04
	2000	30	1.500	0.498	0.200	0.148	0.099	1.395	1.037	0.835	0.444	0.851	9.705e-04
		60	1.499	0.499	0.198	0.144	0.097	1.396	1.044	0.797	0.655	0.617	7.370e-05
		90	1.499	0.501	0.200	0.146	0.099	1.396	1.046	0.729	0.666	0.623	1.339e-04
Actual			1.500	0.500	0.200	0.150	0.100	1.396	1.047	0.785	0.628	0.523	

Tables 2-5 show the performance of SSA, AOA, GWO, RSA, SCA, and WOA for best-estimated weights and corresponding best fitness values for all noise levels. Table 2 shows the best-estimated weights and best fitness value for Ne = 20dB. Similarly, Table 3-5 shows the best-estimated weights and best fitness values for N_e = 40dB, N_e = 60dB, and N_e = 80dB, respectively. Moreover, it can be observed that SSA outperformed the other corresponding optimization algorithms AOA, GWO, RSA, SCA, and WOA, for the developed system model.

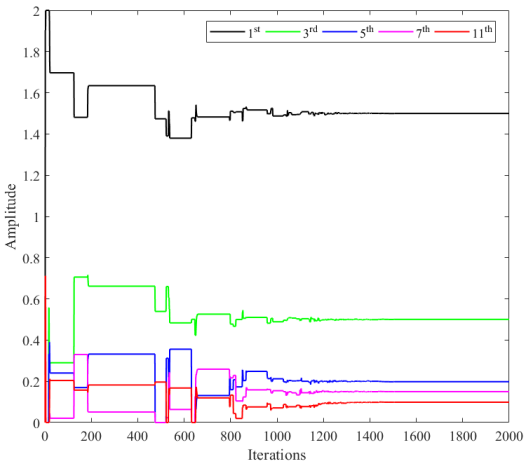
Fig. 14 shows the weighted amplitude plots of the harmonic signal for SSA for all noise levels. Fig. 14 (a) shows the weight amplitude plot for N_e = 20dB noise level. Similarly, Fig. 14(b-d) shows the weighted amplitude plot for N_e = 40dB, N_e = 60dB, and N_e = 80dB, respectively. Moreover, it can be observed in Fig. 14 (a-d) that when the noise level increases, the values of harmonics are affected significantly.



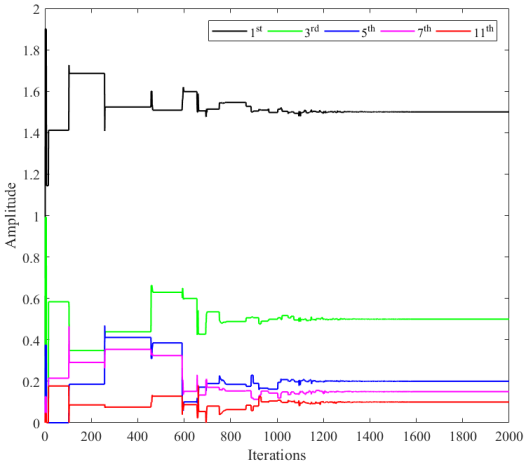
(a) N_e=20dB



(b) N_e=40dB



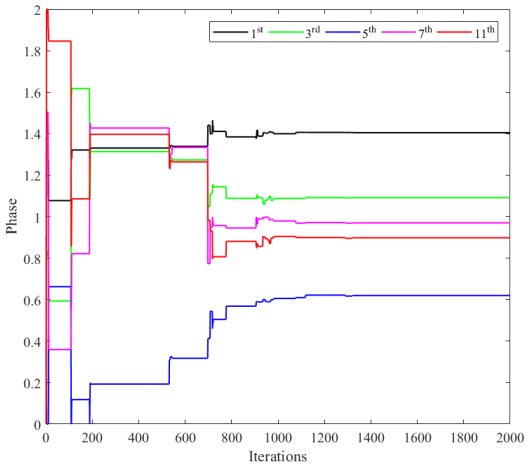
(c) N_e=60dB



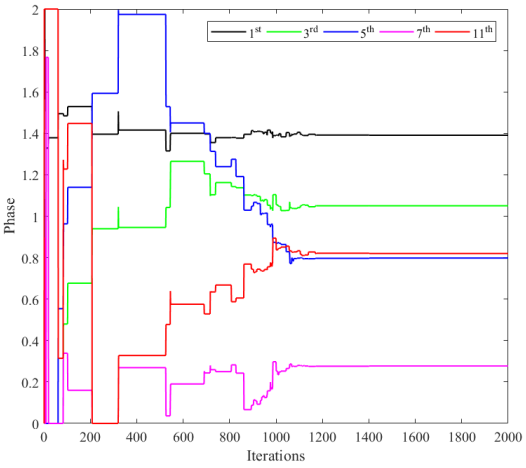
(d) N_e=80dB

Fig. 14 SSA analysis of amplitudes w.r.t. noise levels

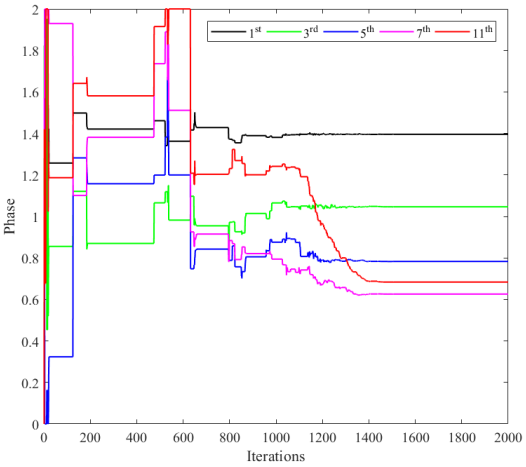
Consequently, Fig. 15 shows the weighted phase plots of the harmonic signal for SSA for all noise levels. Specifically, Fig 15 (a) shows the weighted phase plot for N_e = 20dB noise level. Similarly, Fig. 15(b-d) shows the weighted amplitude plot for Ne = 40dB, N_e = 60dB, and N_e = 80dB, respectively. Moreover, it can be observed from Fig 15 (a-d) that when the noise level increases, the values of harmonics are affected significantly.



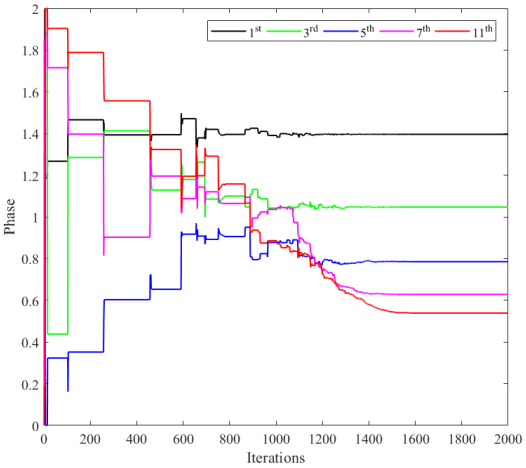
(a) N_e=20dB



(b) N_e=40dB



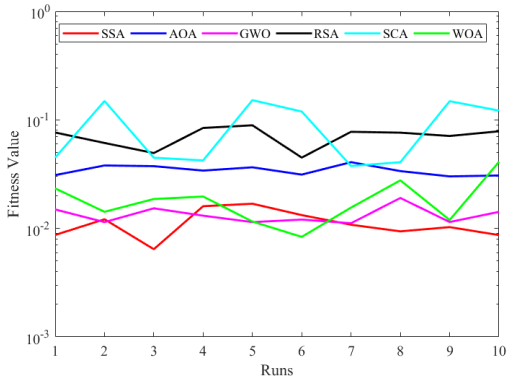
(c) N_e=60dB



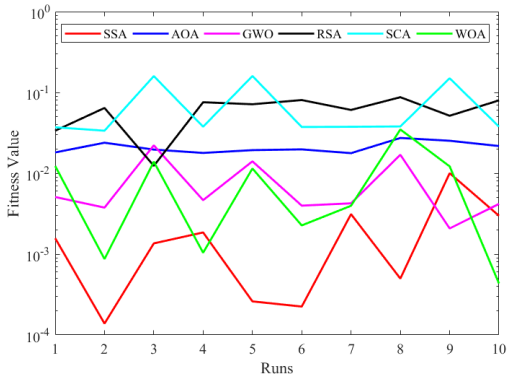
(d) N_e=80dB

Fig. 15 SSA analysis of phases w.r.t. noise levels

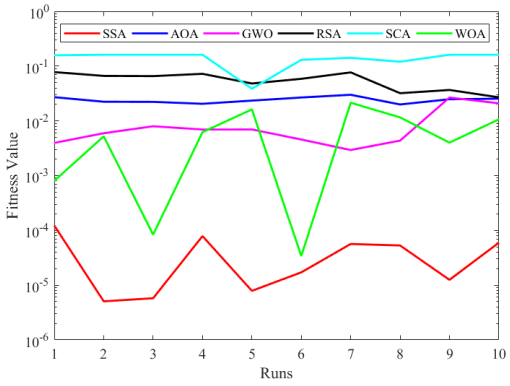
The statistical performance of SSA, AOA, GWO, RSA, SCA, and WOA is shown in Fig 16. Fig. 16(a) shows the statistical performance of all methods/techniques for N_e = 20dB at Pn = 90 and I_t = 2000. Similarly, Fig 16 (b-d) depicts the performance for N_e = 40dB, N_e = 60dB, and N_e = 80dB, respectively. It can be seen from Fig 16 (a-d) that SSA achieves better performance than AOA, GWO, RSA, SCA, and WOA for all independent runs.



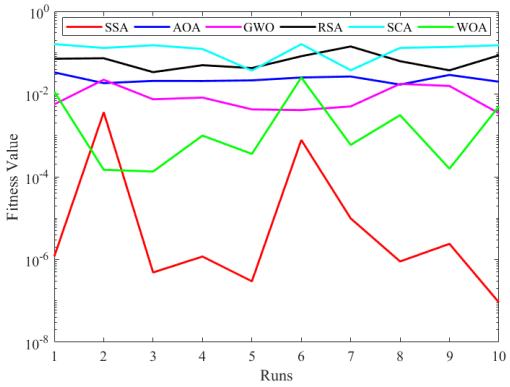
(a) N_e=20dB



(b) N_e=40dB

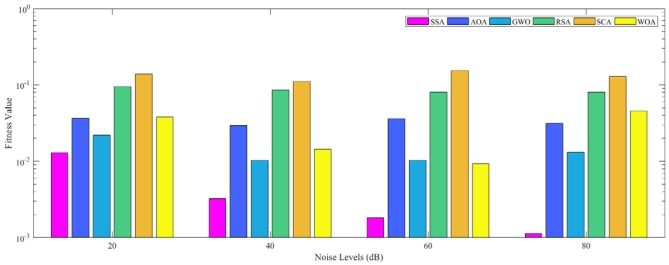


(c) N_e=60dB

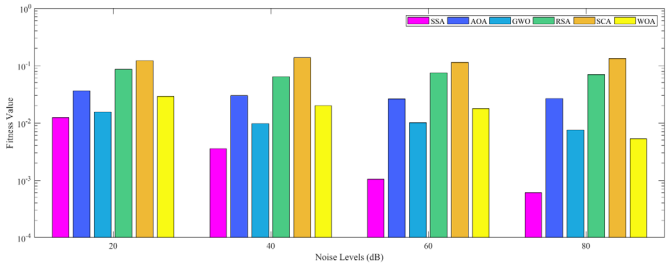


(d) N_e=80dB

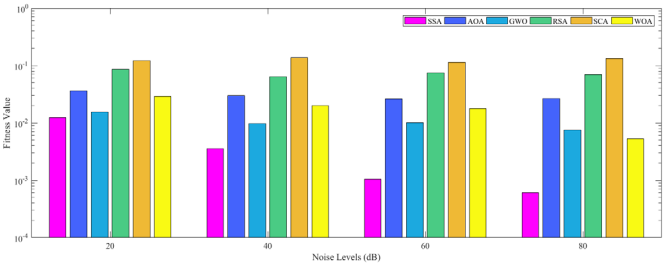
Fig. 16 Statistical plots of SSA, AOA, GWO, RSA, SCA, and WOA w.r.t. noise levels



(a) I_t=500



(b) I_t=1000



(c) I_t=2000

Fig. 17 Average fitness of techniques w.r.t iterations for HPE model

Average fitness plots of SSA, AOA, GWO, RSA, SCA, and WOA for all variations is shown in Fig. 17. Fig 17(a) shows the average fitness values for all noise level at I_t = 500. Similarly, Fig 18(b-c) shows the average fitness values for all noise levels at I_t = 1000, and I_t = 2000, respectively. It is shown in Fig. 17 (a-c) that the average fitness value of SSA is lowest against AOA, GWO, RSA, SCA, and WOA.

5. CONCLUSION

Modern and smart power systems entail an instantaneous estimation and elimination of harmonic signals present in the power system that significantly degrade power quality. Therefore, this paper has exploited an intelligent and sophisticated bio-inspired optimization of SSA to estimate harmonics in modern and smart power systems integrated with renewable energy systems. The estimation of phase, amplitude, and weights are carried out by the SSA and compared with other state-of-the-art optimization heuristics i.e. AOA, GWO, RSA, SCA, and WOA. The analysis is carried out for several I_t = [500. 1000. 2000], P_n = [30, 60, 90] and N_e = [20dB, 40dB, 60dB, 80dB]. The analysis of simulation results depicts that the SSA performance is significantly better for all numbers of iterations, populations, and noise levels compared to AOA, GWO, RSA, SCA, and WOA. Moreover, future studies can be extended towards wearable sensors [42], health care monitoring systems [43], power converter [44], permanent magnet machines [45].

Conflicts of Interest: The authors declare no conflict of interest.

REFERENCES

[1] Fakhar, A., Haidar, A. M., Abdullah, M. O., & Das, N. (2023). "Smart grid mechanism for green energy management: a comprehensive review." *International Journal of Green Energy,* **20**(3), 284-308.

[2] Cheema, K. M. (2020). "A comprehensive review of virtual synchronous generator." *International journal of electrical power & energy systems,* **120**, 106006.

[3] Zhang, C., Lu, W., Xu, Z., & Xue, W. (2023). "Evaluating power system reform proposals based on the evidential reasoning algorithm with hesitant fuzzy information." *Applied Intelligence,* **53**(21), 26079-26097.

[4] Kontargyri, V. T., Tsekouras, G. J., Prousalidis, J. M., Tsirekis, C. D., Leontaritis, K., Alexandris, J. C., ... & Moronis, A. X. (2023). "Comparison of different configurations for shoreline pond electrode station for hvdc transmission systems—part i: electric field study for frames of linear electrode arrangement based on a simplified analytical model." *Applied Sciences,* **13**(12), 7136.

[5] Taghvaie, A., Warnakulasuriya, T., Kumar, D., Zare, F., Sharma, R., & Vilathgamuwa, D. M. (2023). "A comprehensive review of harmonic issues and estimation techniques in power system networks based on traditional and artificial intelligence/machine learning." *Ieee Access,* **11**, 31417-31442.

[6] Ali, S., Bhargava, A., Saxena, A., & Kumar, P. (2023). "A hybrid marine predator sine cosine algorithm for parameter selection of hybrid active power filter." *Mathematics,* **11**(3), 598.

[7] Khajuria, R., Yelisetti, S., Lamba, R., & Kumar, R. (2024). "Optimal model parameter estimation and performance analysis of PEM electrolyzer using modified honey badger algorithm." *International Journal of Hydrogen Energy,* **49**, 238-259.

[8] Peng, Y., Sun, K., He, S., & Alamodi, O. A. (2019). "The influence of samples on meta-heuristic algorithm for parameter estimation of chaotic system." *Modern Physics Letters B,* **33**(04), 1950041.

[9] Mehmood, K., Chaudhary, N. I., Cheema, K. M., Khan, Z. A., Raja, M. A. Z., Milyani, A. H., & Alsulami, A. (2023). "Design of nonlinear marine predator heuristics for hammerstein autoregressive exogenous system identification with key-term separation." *Mathematics,* **11**(11), 2512.

[10] Wang, Z., Wu, D., Wang, Y., & Ji, Z. (2017). "Stochastic gradient identification algorithm for nonlinear system modeling in wind power curtailment prediction." *Modern Physics Letters B,* **31**(19-21), 1740057.

[11] Lobos, T., Kozina, T., & Koglin, H. J. (2001). "Power system harmonics estimation using linear least squares method and SVD." *IEE Proceedings-Generation, Transmission and Distribution,* **148**(6), 567-572.

[12] Heymann, F., Quest, H., Garcia, T. L., Ballif, C., & Galus, M. (2024). "Reviewing 40 years of artificial intelligence applied to power systems–A taxonomic perspective." *Energy and AI,* **15**, 100322.

[13] Javorskyj, I., Yuzefovych, R., Matsko, I., & Zakrzewski, Z. (2022). "The least square estimation of the basic frequency for periodically non-stationary random signals." *Digital Signal Processing,* **122**, 103333.

[14] Xi, J., & Chicharo, J. F. (1996). "A new algorithm for improving the accuracy of periodic signal analysis." *IEEE Transactions on Instrumentation and Measurement,* **45**(4), 827-831.

[15] Jing, F., Liang, J., Wang, Y., & Chen, P. (2023). "Harmonics and intermodulation products-based fuzzy logic (HIPBFL) algorithm for vital sign frequency estimation using a UWB radar." *Expert Systems with Applications,* **228**, 120294.

[16] Alghamdi, T. A., Abdusalam, O. T., Anayi, F., & Packianather, M. (2023). "An artificial neural network based harmonic distortions estimator for grid-connected power converter-based applications." *Ain Shams Engineering Journal,* **14**(4), 101916.

[17] Styvaktakis, E., Bollen, M. H., & Gu, I. Y. (2002). " Expert system for classification and analysis of power system events." *IEEE Transactions on power delivery,* **17**(2), 423-428.

[18] Pradhan, A. K., Routray, A., & Basak, A. (2005). "Power system frequency estimation using least mean square technique." *IEEE transactions on power delivery,* **20**(3), 1812-1816.

[19] Abdelsalam, A. A., Eldesouky, A. A., & Sallam, A. A. (2012). "Characterization of power quality disturbances using hybrid technique of linear Kalman filter and fuzzy-expert system." *Electric power systems Research,* **83**(1), 41-50.

[20] Chudamani, R., Vasudevan, K., & Ramalingam, C. S. (2009). "Non-linear least-squares-based harmonic estimation algorithm for a shunt active power filter." *IET Power Electronics,* **2**(2), 134-146.

[21] Dhineshkumar, K., Subramani, C., & Prakash, G. (2018). "Kalman filter algorithm for mitigation of power system harmonics." *International Journal of Electrical and Computer Engineering,* **8**(2), 771-779.

[22] Singh, S. K., Sinha, N., Goswami, A. K., & Sinha, N. (2016). "Several variants of Kalman Filter algorithm for power system harmonic estimation." *International Journal of Electrical Power & Energy Systems,* **78**, 793-800.

[23] Xu, W., Huang, C., & Jiang, H. (2021). "Analyses and enhancement of linear Kalman-filter-based phase-locked loop." *IEEE Transactions on Instrumentation and Measurement,* **70**, 1-10.

[24] Wang, Y., Huang, S., & Ji, Z. (2017). "Operation management of daily economic dispatch using novel hybrid particle swarm optimization and gravitational search algorithm with hybrid mutation strategy." *Modern Physics Letters B*, **31**(19-21), 1740099.

[25] Mehmood, K., Chaudhary, N. I., Khan, Z. A., Cheema, K. M., Raja, M. A. Z., Alshamrani, S. S., & Alshmrany, K. M. (2025). "Design of chaos induced Aquila optimizer for parameter estimation of electro-hydraulic control system." *CMES-Computer Modeling in Engineering and Sciences,* **143**(2), 1809-1841.

[26] Mehmood, K., Chaudhary, N. I., Khan, Z. A., Cheema, K. M., & Raja, M. A. Z. (2025). "Design of quantum computing-based avain navigation optimization algorithm for parameter estimation of input nonlinear output error model with key term separation." *Modern Physics Letters A,* **40**(11n12), 2550019.

[27] Cheema, K. M., Mehmood, K., Chaudhary, N. I., Khan, Z. A., Raja, M. A. Z., El-Sherbeeny, A. M., & Nadeem, A. (2024). "Knacks of marine predator heuristics for distributed energy source-based power systems harmonics estimation." *Heliyon, **10***(15).

[28] Mehmood, A., Shi, P., Raja, M. A. Z., Zameer, A., & Chaudhary, N. I. (2021). "Design of backtracking search heuristics for parameter estimation of power signals." *Neural Computing and Applications,* **33**(5), 1479-1496.

[29] Cheema, K. M., Mehmood, K., Chaudhary, N. I., Khan, Z. A., Raja, M. A. Z., & Nadeem, A. (2024). "Knacks of evolutionary mating heuristics for renewable energy Source–Based power systems signal harmonics Estimation." *International Journal of Energy Research,* **2024**(1), 8871266.

[30] Malik, N. A., Chang, C. L., Chaudhary, N. I., Raja, M. A.

Z., Cheema, K. M., Shu, C. M., & Alshamrani, S. S. (2022). "Knacks of fractional order swarming intelligence for parameter estimation of harmonics in electrical systems." *Mathematics,* **10**(9), 1570.

[31] Mehmood, K., Chaudhary, N. I., Khan, Z. A., Cheema, K. M., & Raja, M. A. Z. (2023). "Parameter estimation of nonlinear systems: Dwarf mongoose optimization algorithm with key term separation principle." *Journal of Ambient Intelligence and Humanized Computing,* **14**(12), 16921-16931.

[32] Malik, N. A., Chang, C. L., Chaudhary, N. I., Khan, Z. A., Zahoor Raja, M. A., Kiani, A. K., ... & Azhari, A. A. (2022). "Parameter estimation of harmonics arising in electrical instruments of smart grids using cuckoo search heuristics." *Frontiers in Energy Research,* **10**, 1059132.

[33] Ismael, S. M., Aleem, S. H. A., Abdelaziz, A. Y., & Zobaa, A. F. (2019). "State-of-the-art of hosting capacity in modern power systems with distributed generation." *Renewable energy,* **130**, 1002-1020.

[34] Pandey, S. K., Mohanty, S. R., & Kishor, N. (2013). "A literature survey on load–frequency control for conventional and distribution generation power systems." *Renewable and Sustainable Energy Reviews,* **25**, 318-334.

[35] Ahmed, E. M., Rakočević, S., Ćalasan, M., Ali, Z. M., Hasanien, H. M., Turky, R. A., & Aleem, S. H. A. (2022). "BONMIN solver-based coordination of distributed FACTS compensators and distributed generation units in modern distribution networks." *Ain Shams Engineering Journal,* **13**(4), 101664.

[36] Cheema, K. M., Chaudhary, N. I., Tahir, M. F., Mehmood, K., Mudassir, M., Kamran, M., ... & Elbarbary, Z. S. (2022). "Virtual synchronous generator: Modifications, stability assessment and future applications." *Energy Reports*, **8**, 1704-1717.

[37] Malik, N. A., Chaudhary, N. I., & Raja, M. A. Z. (2023). "Firefly optimization heuristics for sustainable estimation in power system harmonics." *Sustainability,* **15**(6), 4816.

[38] Anwar, N., Shahzadi, K., Raja, M. A. Z., Ahmad, I., Shoaib, M., & Kiani, A. K. (2026). "Machine intelligent expedition with supervised Bayesian adaptive neural networks for stochastic cholera epidemic model in a periodic environment: N. Anwar et al." *Nonlinear Dynamics,* **114**(2), 141.

[39] Anwar, N., Shahzadi, K., Raja, M. A. Z., Ahmad, I., Shoaib, M., & Kiani, A. K. (2025). "Machine learning expedition with nonlinear ARX neural networks for wiener stochastic differential system in cancer virotherapy with impact of immune response." *Fluctuation and Noise Letters,* **24**(06), 2550062.

[40] Anwar, N., Raja, M. A. Z., Kiani, A. K., Ahmad, I., Shoaib, M., & Shu, C. M. (2025). "Stochastic adaptive autoregressive eXogenous networks operative with Grünwald Letnikove fractional finite differences for nonlinear fractal differential system of coffee rust control model." *International Journal of Computer Mathematics,* **102**(10), 1639-1680.

[41] Anwar, N., Naz, S., Raja, M. A. Z., Ahmad, I., Shoaib, M., & Kiani, A. K. (2025). "Machine learning solutions with supervised adaptive neural networks for countermeasure competing strategy of computer virus models." *Simulation Modelling Practice and Theory,* **142**, 103141.

[42] Naveed, F., Khan, H., Uddin, Z., Cheema, K. M., Khan, M. F., & Ahmed, S. S. (2026). "Human activity recognition using CNN–BiLSTM with attention on hip-mounted wearable sensors." *Scientific Reports.*

[43] Elbarbary, Z. S., Cheema, K. M., Al-Gahtani, S. F., & El-Sehiemy, R. A. (2022). "High gain chopper supplied from PV system to fed synchronous reluctance motor drive for pumping water application." *Scientific Reports,* **12**(1), 15519.

[44] Xu, Z., Din, Z., Jiang, Y., Cheema, K. M., Milyani, A. H., & Alghamdi, S. (2022). "High-resistance connection diagnosis considering current closed-loop effect for permanent magnet machine." *Frontiers in Energy Research,* **10**, 933246.

[45] Ullah, B., Khan, F., Qasim, M., Khan, B., Milyani, A. H., Cheema, K. M., & Din, Z. (2021). "Lumped parameter model and electromagnetic performance analysis of a single-sided variable flux permanent magnet linear machine." *Energies,* **14**(17), 5494.